ChemComm

COMMUNICATION

View Article Online
View Journal | View Issue

Cite this: *Chem. Commun.*, 2015, **51**, 3336

Received 1st December 2014,
Accepted 7th January 2015

DOI: 10.1039/c4cc09569c

www.rsc.org/chemcomm

Polyoxometalates-based heterometallic organic–inorganic hybrid materials for rapid adsorption and selective separation of methylene blue from aqueous solutions†

Fei-Yan Yi,‡[a] Wei Zhu,‡[b] Song Dang,[a] Jian-Ping Li,[b] Dai Wu,[b] Yun-hui Li[b] and Zhong-Ming Sun*[a]

A series of LnCu–polyoxometalates (POMs) were used for dye-wastewater treatment with rapid (within 1 min) and large-scale adsorption (up to 391.3 mg g^{-1}) as well as excellent selective separation of cationic dyes. Furthermore, the adsorbed dyes can be easily desorbed, and the POMs still work very efficiently even after three cycles.

In daily life, a large amount of dye-wastewater discharged poses a significant threat to the aqueous environment and human health due to its toxicity and even carcinogenicity.[1] Therefore, the removal of these dyes is extremely important, but it will be more attractive if the recovery and recycling of raw materials can be realized at the same time, which is considerably challenging. In this regard, a low-cost and eco-friendly adsorption technology was considered to be more competitive[2,3] than some other methods such as photocatalytic degradation, and so on.[4,5] Activated carbon, as a traditional adsorbent in the treatment of dye-wastewater, is only effective for wastewater containing low concentrations of dye,[6] and it has poor dye specificity due to its neutral framework. Thus, it is necessary to find a desirable adsorption material, which not only is able to reduce the pollutant organic dyes with high efficiency and low loss, but also realizes selective separation and recovery of raw materials. Polyoxometalates (POMs)-based organic–inorganic hybrid material may be a suitable choice. POMs, as an outstanding family of metal-oxide clusters[7,8] with controllable shape and size, highly electronegative, and oxo-enriched surfaces, are expected to exhibit good adsorption and selective separation towards cationic dyes because they may have a stronger attraction to cationic dyes than anionic dyes. Wang's group recently reported a POM@MOF composite material, which demonstrates that various POMs incorporated into MIL-101 can improve the adsorption capacity for dyes.[12] POMs-based hybrid materials as adsorption materials still have not been explored up to now, although they exhibit great potential for applications in various fields.[9–11] With this in mind, we intend to design and synthesize novel POMs-based hybrid materials, and then further investigate their adsorption and regeneration behaviour for dye molecules from wastewater.

In this study, a series of new organic–inorganic hybrid monovacant Keggin-type silicotungstates (LnCu–POMs) containing 3d–4f lanthanide^{III}–Cu^{II} heterometallic cations were hydrothermally synthesized with a mixture containing $K_8[\alpha\text{-}SiW_{11}O_{39}]\cdot 13H_2O$, $CuCl_2\cdot 2H_2O$, $LnCl_3\cdot 6H_2O$ (Ln = Dy, **1** and **2**; Er, **3** and **4**) and en (**1–3**) (or DETA (**4**)) [en = ethylenediamine, DETA = diethylenetriamine], and further characterized by PXRD, FTIR, and thermogravimetric analyses (TGA). The compounds **2** and **3** were obtained when oxalic acid was respectively added in the reaction mixtures used for **1** with en and **4** with DETA. It is well known in POMs systems that the reaction pH values strongly affect the formation of various structure types.[13] Single-crystal X-ray diffraction analyses (Table S1, ESI†) reveal that compounds **Dy-1** and **Er-4** crystallize in the monoclinic space group *Cm* and $P2_1c$, respectively. Compounds **Dy-2** and **Er-3** are isostructural and crystallize in the orthorhombic space group *Fdd*2. Based on elemental analyses, single-crystal X-ray diffraction, thermogravimetric analyses (TGA), and charge-balance considerations (see the ESI†), their formula were confirmed as $[K_2(H_2O)_{6.5}][Cu(en)_2]_2[Dy(H_2O)_2SiW_{11}O_{39}]_2\cdot[Cu(H_2O)(en)_2]_2\cdot 10H_2O$ (**Dy-1**), $[Cu(en)_2]_3[Ln(H_2O)SiW_{11}O_{39}]_2(C_2O_4)\cdot[Cu(H_2O)(en)_2]_3\cdot 10H_2O$ (Ln = **Dy-2**, **Er-3**), $[Cu(H_2O)(DETA)_2]H_{11}[Er(SiW_{11}O_{39})_2]\cdot 2DETA\cdot 6H_2O$ (**Er-4**). Their asymmetric units contain lacunary $[\alpha\text{-}SiW_{11}O_{39}]^{8-}$ POMs, in which a lanthanide cation occupies the vacant site and connects the terminal oxygen atoms of the POMs. Considering the charge balance, some protons should be added to **Er-4**. To locate the positions of these protons, bond valence sum (BVS) calculations[14] have been performed on all the atoms of the POMs framework. The results show that all Si, W and Er atoms are in their formal valences of +4, +6 and +3, respectively. Except that

[a] *State Key Laboratory of Rare Earth Resource Utilization, Changchun Institute of Applied Chemistry, Chinese Academy of Sciences, 5625 Renmin Street, Changchun, Jilin 130022, China. E-mail: szm@ciac.ac.cn; Web: http://zhongmingsun.weebly.com*
[b] *School of Chemistry & Environmental Engineering, Changchun University of Science & Technology, Changchun 130022, China*

† Electronic supplementary information (ESI) available: X-ray crystallographic cif files, materials and methods, crystal data, structural information, and characterization data including PXRD patterns, IR, TGA, UV-vis spectra and digital images for the adsorption of dyes. CCDC 1028827–1028829. For ESI and crystallographic data in CIF or other electronic format see DOI: 10.1039/c4cc09569c

‡ These authors contributed equally.

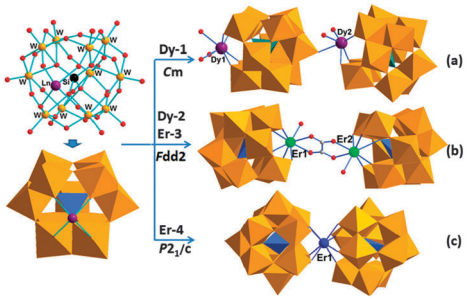

Fig. 1 The asymmetrical molecular polyhedral representation of LnPOMs building units in **1** (a), **2** and **3** (b), and **4** (c). Color mode: gold octahedra, WO_6; blue tetrahedra, SiO_4; red spheres, O; grey spheres, C.

the BVS values (1.60 for O5, 1.54 for O46, 1.60 for O58, 1.60 for O92, 1.57 for O93 and 1.54 for O95) in **Er-4** are significantly lower than 2 (Table S2, ESI†), indicating they may be monoprotonated, the other O atoms are in the oxidation states of −2.

The molecular unit of **Dy-1** consists of one $[K_2(H_2O)_{6.5}]^{2+}$ dimer, two unique $[Dy(H_2O)_2SiW_{11}O_{39}]^{5-}$ polyanions, two coordinated $[Cu(en)_2]^{2+}$, two discrete $[Cu(H_2O)(en)_2]^{2+}$ and ten water molecules of crystallization (Fig. S1, ESI†). Two coordinated $[Cu(en)_2]^{2+}$ cations link to the Dy–POMs fragment *via* its terminal oxygen atoms. All Cu^{2+} ions locate on the special sites with 50% occupancy and adopt the square pyramid geometry with four N atoms from two en ligands and one oxygen atom from $[Dy(H_2O)_2(SiW_{11}O_{39})]^{5-}$ or one aqua ligand. The neighboring $[Dy(H_2O)_2(SiW_{11}O_{39})]^{5-}$ polyanion units are bridged into a one-dimensional chain structure by $[Dy(H_2O)_2]^{3+}$ and $[K_2(H_2O)_{6.5}]$ dimers (Fig. 1 and Fig. S1, ESI†). Each Dy^{3+} is seven-coordinate with two coordinated oxygen atoms from water molecules and five from two $[SiW_{11}O_{39}]^{8-}$ fragments. The crystal structures of **Dy-2** and **Er-3** also contain two similar POMs fragments $[Ln(H_2O)(SiW_{11}O_{39})]^{5-}$, three linked $[Cu(en)_2]^{2+}$ ions, three discrete $[Cu(H_2O)(en)_2]^{2+}$ ions, one $\{C_2O_4\}^{2-}$ ion and ten lattice water molecules (Fig. S2, ESI†). The difference is that, in **2** and **3**, such $[Ln(H_2O)(SiW_{11}O_{39})]^{5-}$ polyanion fragments were linked into a large Ln–POMs dimer cluster by $\{C_2O_4\}^{2-}$ ligands in face-to-face mode (Fig. 1b). However, two monovacant $[SiW_{11}O_{39}]^{8-}$ fragments in **Er-4** were connected by an eight-coordinate Er^{3+} cation into a well-known sandwich-type $\{[SiW_{11}O_{39}]^{8-}–Er–[SiW_{11}O_{39}]^{8-}\}$ structure (Fig. 1 and Fig. S3, ESI†). The Er^{3+} coordination cation adopts a distorted square antiprismatic geometry. Free water molecules are filled in the space among the POMs. Finally, 3D extended supramolecular architectures for **1–4** were formed in view of hydrogen bonding interactions between nitrogen atoms of en or DETA molecules and surface oxygen atoms of POM fragments or water molecules. The experimental PXRD patterns for **1–4** are in good agreement with the simulated patterns from the single-crystal X-ray diffraction, demonstrating the good phase purities for **1–4**.

To evaluate the adsorption ability of **Dy-1**, **Dy-2**, **Er-3** and **Er-4** for the removal of dye from contaminated water, methylene blue (MB), methyl orange (MO) and rhodamine-B (RhB) with different charges and sizes as the typical organic pollutant targets were selected for experiments. The digital images and UV-vis spectroscopic results show that the removal of MO and RhB dyes is almost negligible for **1–4** (Fig. S4, ESI†), but MB dye is almost completely adsorbed.

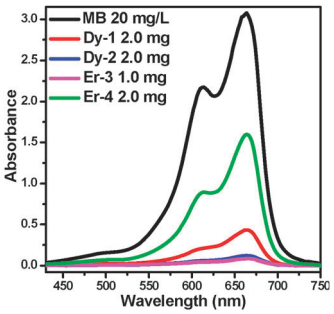

Fig. 2 The adsorption capability of **1–4** toward MB dyes.

To systematically investigate the adsorption behavior of the four compounds towards MB dye, the UV-vis absorption spectra of MB dye solution (20 mg L^{-1}, 20 mL) in the presence of **1–4** with different concentrations and constant time were compared. As shown in Fig. 2 and Fig. S5 (ESI†), the removal efficiency of **Er-3** is the best and MB has been almost completely adsorbed with 1 mg of **Er-3**. The order of adsorption efficiency is **Er-3** > **Dy-2** > **Dy-1** > **Er-4**. The UV-vis spectra of pure MB solution with different concentrations was also obtained and used to determine the uptake capacity of four compounds (Fig. S6, ESI†). The uptake capacities of 193.6 mg g^{-1} for **Dy-1**, 218 mg g^{-1} for **Dy-2**, 391.3 mg g^{-1} for **Er-3**, and 114.3 mg g^{-1} for **Er-4** were achieved at room temperature. These uptake capacities are considerably higher than that of commercial activated carbon[6b] and also considerably high compared to that of other materials reported up to now (Table 1).

Fast adsorption rate, such that a material can remove most of the targeted dyes in a short time, is also a very important parameter to assess the efficiency and practicability of adsorbent in an economical wastewater disposal system. It is a very exciting discovery that the adsorption rate for **Dy-1** reached to 90% in 1 min (Fig. 3a), and adsorption is almost complete in 15 min; compounds **Dy-2** and **Er-3** also completely remove MB molecules in 1 h (Fig. 3b and Fig. S7, ESI†). These results revealed that they were efficiently able to remove the MB molecules.

As can be seen from the abovementioned experiments, compounds **1–4** clearly exhibit superior adsorption properties for MB dyes compared with MO and RhB dye molecules. As expected, a large number of negative charges on the surface of the four LnCu–POMs may cause them to preferentially adsorb cationic MB-dye rather than anionic MO dye. Such a rapid adsorption rate for **Dy-1** towards MB dyes was suspected to be due to the large amounts of dye adsorbed on the surface of sample particles. However, such an assumption does not explain why RhB with the same positive charge represents little uptake capacity. To deeply understand the removal

Table 1 Comparison of MB adsorption capacity in various materials

Materials	Adsorption capacity (mg g^{-1})	Ref.
Activated carbon	135	6*b*
Graphene oxide	397	3*a*
MOF@graphite oxide	18	3*b*
Zn-DDQ	135	3*d*
Zn-MOF	0.75	3*e*
$PW_{11}V$@MIL-101	371	12
ErCu–POM (**Er-3**)	391.3	This work

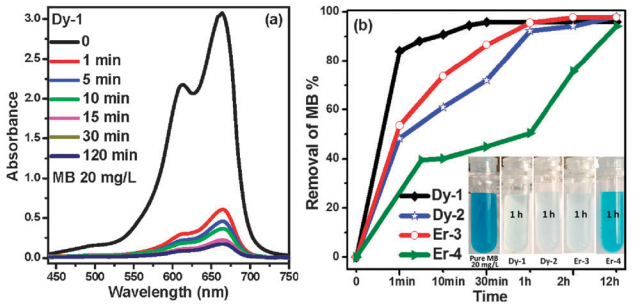

Fig. 3 (a) The adsorption rate with **Dy-1** at various contact time. (b) The corresponding removal efficiency of MB over **1** (black), **2** (blue), **3** (red), **4** (olive) as well as visual images of pure MB and MB@**1–4** at 1 h.

process of dyes and clarify that they were adsorbed on the surface of sample particles or exchanged into the interior of crystals, a series of detailed studies have been performed. The solid particles and upper clear solution after the adsorption of MB dye by **Dy-1** were analyzed *via* elemental analysis (EA) of S as well as inductively coupled plasma (ICP) spectrometry for Cu and K. EA results indicate an S amount of about 0.52% (slightly more than one MB cation) can be detected, which is considerably smaller than the experimental result (2.17%, 4.7 MB cations). ICP results (Cu, 16.6 μg mL^{-1}; K, 9.6 μg mL^{-1}) for the upper clear solution are considerably in accordance with the structural information of **Dy-1** containing two isolated $[Cu(H_2O)(en)_2]^{2+}$ (a half of 36.7 μg mL^{-1} based on all Cu) and two K^+ ions (total 11.3 μg mL^{-1} based on K). In contrast, **Dy-1** was immersed into the aqueous solution for 24 h, and then the upper clear solution was also analyzed by ICP. The result is that Cu and K are not detected. The abovementioned analyses confirm that the adsorption for **Dy-1** towards MB dye is indeed an ion-exchange process, where the free cations of K^+ and $[Cu(en)_2]^{2+}$ can be released during the adsorption of MB, and the adsorbed MB molecules may be exchanged into the interior of the **Dy-1** crystal. At the same time, to balance the changes, about five MB cations in theory may be adsorbed by **Dy-1**, *i.e.*, one **Dy-1** molecule may adsorb five MB cations; thus, the adsorption quantity for **Dy-1** is about 20.6%, which is very close to the experimental result (19.35%). However, the pore volume ratio for **Dy-1** is 18.8% based on the calculation performed using the PLATON program,[15] and the corresponding total potential solvent accessible void volume is 1166.8 $Å^3$ out of the 6209.3 $Å^3$ unit cell volume. However, the molecular volume of MB is ~419.9 $Å^3$, and thus most of the ~2.7 mol MB cations may be ideally inserted into the void space of **Dy-1**. Combining the EA result of S in the interior of crystals after adsorption, it could be inferred that most of the adsorbed MB molecules should be on the surface of sample particles. From the experimental results and structural information of **1–4**, the amounts of negative charges on the surface for **1–4** play a key role in the adsorption process. Omitting the isolated cationic part, the CuDy–POMs of **Dy-1** represents 4 negative charges, CuEr–POMs of **Er-3** contains 6 negative charges, and CuEr–POM of **Er-4** contains 3 negative charges, which is consistent with the experimental order of adsorption efficiency and capacity of the target compounds (**Er-3** > **Dy-1** > **Er-4**) towards MB dyes. Thus, the anionic MO can be not naturally adsorbed. To further investigate the reason of negligible adsorption for RhB with positive changes, another cationic dye, basic red 2 (BR2) with similar size but different functional groups (Fig. S8, ESI†), has been selected for a comparative experiment. As shown in Fig. S9 (ESI†), the UV-vis spectra of the aqueous solution of BR2 (20 mg L^{-1}) dye with **Dy-1** for the given time interval as well as with different compounds **Dy-2**, **Er-3** and **Er-4** indicate that the adsorption of BR2 with **1–4** was negligible. The ICP data of the upper solution after adsorption for **Dy-1** towards RhB and BR2 dyes show that K^+ and Cu^{2+} from the $[Cu(en)_2]^{2+}$ are almost not detected. The result further confirms that the ion-exchange is the key for the occurrence of adsorption, although most of the dyes are adsorbed on the surface of the samples. MB molecules with small size may be exchanged into the void space of the crystals, triggering the process, but RhB and BR2 are not due to their large sizes and steric hindrance. Because it is very difficult to *in situ* monitor this adsorption process, the removal mechanism of dyes is still not completely clear at this moment. To further confirm whether **Dy-1**, **Dy-2**, **Er-3** and **Er-4** materials have the ability to separate and recover MB dyes from mixed dye solution, the mixed dye solution of MB and RhB, MB and MO were prepared and used (Fig. 4 and Fig. S10a, ESI†). UV/vis spectra were measured to determine the separation capability of **1–4**, which shows that all the absorption peaks of MB molecules quickly disappeared, just leaving the characteristic absorption peaks of RhB and MO exposed to the corresponding dye-mixture (Fig. 4 and Fig. S10b–i, ESI†). The digital images of dye-selective adsorption clearly shows the color change from green for mixed MB–MO and purple for MB–RhB to pure orange for MO and pink for RhB solution, which can be readily observed by the naked eye (Fig. S10j and k, ESI†). Through the abovementioned discussion, it can be concluded that the materials exhibit excellent selective adsorption ability towards the cationic MB dyes in wastewater.

The stability and reusability of target materials are another important standard for practical application. After adsorption experiments, adsorbents **1–4** can be separated by simple centrifugation due to their insoluble properties in water. When a mixed solution of NaCl with ethanol and H_2O (v : v, 1 : 1) was added, UV-vis spectra and digital images show that MB dye molecules in MB@**Dy-1** can be rapidly released (Fig. 5 and Fig. S11, ESI†). This release process has also been monitored in various other eluting solutions (Fig. S12, ESI†), such as pure water, pure ethanol solution, aqueous solution of NaCl, as well as the mixed solution of NaCl with ethanol and water of different volume ratios (1 : 9 and 9 : 1). These contrastive results show that the MB molecules in MB@**Dy-1** are released the fastest and almost completely in the solution of NaCl with ethanol and H_2O

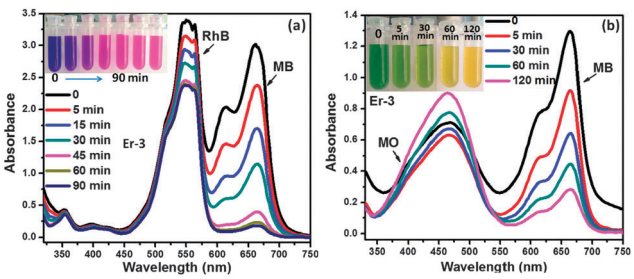

Fig. 4 The selective adsorption capability of **Er-3** toward the mixed dyes: (a) RhB and MB, (b) MO and MB. Inset: the color change of the mixed dyes solution before and after adsorption experiments at given intervals.

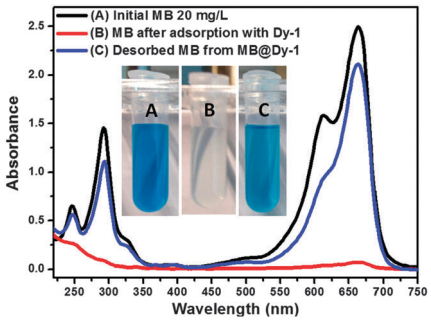

Fig. 5 UV-vis spectra and corresponding digital images of MB solution before (A) and after adsorption experiments (B), as well as the MB released from the MB@**Dy-1** (C).

(v : v, 1 : 1) over other solutions. This means that the dye release is also an ion-exchange process,[16] which also further demonstrates that ionic interaction between dyes and the anionic framework is the main determinant for the selective adsorption and separation of dyes. The ICP data of the MB solution from MB@**Dy-1** after desorption suggests that the Na^+ ions from eluting solution only replace cationic MB molecules because the amounts of K and Cu are negligible. Taking **Dy-1** as an example, three adsorption and desorption cycles with MB solution were further examined. The experimental results show that the adsorption ability of **Dy-1** did not exhibit a significant loss after ad-desorption tests of three cycles (Fig. S13, ESI†). Moreover, the PXRD patterns of the **1–4** regenerated from adsorption and desorption experiments match well with the as-synthesized product (Fig. S14, ESI†), indicating that the structure of the four compounds remain intact, which confirms its good stability and recyclability. In a word, the four LnCu–POMs materials exhibit good reproducibility. Adding their fast adsorption, the foregoing two aspects are of great significance for the practical use of the absorbent.

Four new LnCu–POMs (**1–4**) materials have been successfully synthesized, and were adopted as adsorbents for the removal of dyes in aqueous solution. Interestingly, they not only exhibit rapid adsorption rate and high uptake capacity towards cationic MB dye, but also realize the fast selective separation and recovery of MB dye from the mixed dye-wastewater (RhB and MB, MO and MB) as is expected. Furthermore, they are also reusable. This work opens up a useful, economical adsorption and separation material, which inspires further studies that will be focused on the construction of more novel materials with a large number of charges encapsulated in the surface, which can improve the selective separation and recycling of raw material in wastewater.

Notes and references

1 (*a*) B. Adhikari, G. Palui and A. Banerjee, *Soft Matter*, 2009, **5**, 3452; (*b*) S. Lin, Z. Song, G. Che, A. Ren, P. Li, C. Liu and J. Zhang, *Microporous Mesoporous Mater.*, 2014, **193**, 27; (*c*) W. Fan, W. Gao, C. Zhang, W. W. Tjiu, J. S. Pan and T. X. Liu, *J. Mater. Chem.*, 2012, **22**, 25108.

2 (*a*) M. Tong, D. Liu, Q. Yang, S. Devautour-Vinot, G. Maurinb and C. Zhong, *J. Mater. Chem. A*, 2013, **1**, 8534; (*b*) E. Forgas, T. Cserhati and G. Oros, *Environ. Int.*, 2004, **30**, 953; (*c*) F. Liu, S. Chung, G. Oh and T. S. Seo, *ACS Appl. Mater. Interfaces*, 2012, **4**, 922.

3 (*a*) J.-D. Xiao, L.-G. Qiu, X. Jiang, Y.-J. Zhu, S. Ye and X. Jiang, *Carbon*, 2013, **59**, 372; (*b*) L. Li, X. L. Liu, H. Y. Geng, B. Hu, G. W. Song and Z. S. Xu, *J. Mater. Chem. A*, 2013, **1**, 10292; (*c*) M.-L. Ma, J.-H. Qin, C. Ji, H. Xu, R. Wang, B.-J. Li, S.-Q. Zang, H.-W. Hou and S. R. Batten, *J. Mater. Chem. C*, 2014, **2**, 1085; (*d*) Y. Zhu, Y.-M. Wang, S.-Y. Zhao, P. Liu, C. Wei, Y.-L. Wu, C.-K. Xia and J.-M. Xie, *Inorg. Chem.*, 2014, **53**, 7692; (*e*) C.-Y. Sun, X.-L. Wang, C. Qin, J.-L. Jin, Z.-M. Su, P. Huang and K.-Z. Shao, *Chem. – Eur. J.*, 2013, **19**, 3639.

4 (*a*) M. N. Chong, B. Jin, C. W. K. Chow and C. Saint, *Water Res.*, 2010, **44**, 2997; (*b*) B.-L. Fei, W. Li, J.-H. Wang, Q.-B. Liu, J.-Y. Long, Y.-G. Li, K.-Z. Shao, Z.-M. Su and W.-Y. Sun, *Dalton Trans.*, 2014, **43**, 10005; (*c*) H. Yang, T. Liu, M. Cao, H. Li, S. Gao and R. Cao, *Chem. Commun.*, 2010, **46**, 2429; (*d*) K. Lv and Y. Xu, *J. Phys. Chem. B*, 2006, **110**, 6204; (*e*) Y. Yang, Y. Guo, C. Hu, C. Jiang and E. Wang, *J. Mater. Chem.*, 2003, **13**, 1686.

5 (*a*) S. A. Avlonitis, I. Poulios, D. Sotiriou, M. Pappas and K. Moutesidis, *Desalination*, 2008, **221**, 259; (*b*) A. G. Vlyssides, D. Papaioannou, M. Loizidoy, P. K. Karlis and A. A. Zorpas, *Waste Manage.*, 2000, **20**, 569; (*c*) C. I. Pearce, J. R. Lloyd and J. T. Guthrie, *Dyes Pigm.*, 2003, **58**, 179; (*d*) V. Gómez, M. S. Larrechi and M. P. Callao, *Chemosphere*, 2007, **69**, 1151; (*e*) D. Asma, S. Kahraman, S. Cing and O. Yesilada, *J. Basic Microbiol.*, 2006, **46**, 3.

6 (*a*) A. A. Attia, W. E. Rashwan and S. A. Khedr, *Dyes Pigm.*, 2006, **69**, 128; (*b*) The national standard of the People's Republic of China: wooden granular activated carbon for water purification. GB/T13803.2-1999.

7 (*a*) E. Burkholder, V. Golub, C. J. O'Connor and J. Zubieta, *Inorg. Chem.*, 2003, **42**, 6729; (*b*) H. N. Miras, J. Yan, D.-L. Long and L. Cronin, *Chem. Soc. Rev.*, 2012, **41**, 7403; (*c*) C. Zou, Z. J. Zhang, X. Xu, Q. H. Gong, J. Li and C. D. Wu, *J. Am. Chem. Soc.*, 2012, **134**, 87; (*d*) G. Izzet, M. Ménand, B. Matt, S. Renaudineau, L.-M. Chamoreau, M. Sollogoub and A. Proust, *Angew. Chem., Int. Ed.*, 2012, **51**, 487; (*e*) Y. Kikukawa, Y. Kuroda, K. Yamaguchi and N. Mizuno, *Angew. Chem., Int. Ed.*, 2012, **51**, 2434.

8 (*a*) X.-B. Han, Z.-M. Zhang, T. Zhang, Y.-G. Li, W. Lin, W. You, Z.-M. Su and E.-B. Wang, *J. Am. Chem. Soc.*, 2014, **136**, 5359; (*b*) Z. M. Zhang, S. Yao, Y. G. Li, H. H. Wu, Y. H. Wang, M. Rouzières, R. Clérac, Z. M. Su and E.-B. Wang, *Chem. Commun.*, 2013, **49**, 2515; (*c*) N. V. Izarova, M. T. Pope and U. Kortz, *Angew. Chem., Int. Ed.*, 2012, **51**, 9492; (*d*) T. Yamase, *Chem. Rev.*, 1998, **98**, 307; (*e*) U. Kortz, A. Müller, J. van Slageren, J. Schnack, N. S. Dalal and M. Dressel, *Coord. Chem. Rev.*, 2009, **253**, 2315.

9 (*a*) C. L. Hill, *Chem. Rev.*, 1998, **98**, 1; (*b*) M. P. Pope and A. Müller, *Polyoxometalate Chemistry: From Topology via Self-Assembly to Applications*, Kluwer, Dordrecht, The Netherlands, 2001; (*c*) A. Dolbecq, E. Dumas, C. R. Mayer and P. Mialane, *Chem. Rev.*, 2010, **110**, 6009; (*d*) S. G. Mitchell, C. Streb, H. N. Miras, T. Boyd, D.-L. Long and L. Cronin, *Nat. Chem.*, 2010, **2**, 308; (*e*) P. Yin, J. Wang, Z. Xiao, P. Wu, Y. Wei and T. Liu, *Chem. – Eur. J.*, 2012, **18**, 9174.

10 (*a*) X. Kuang, X. Wu, R. Yu, J. P. Donahue, J. Huang and C.-Z. Lu, *Nat. Chem.*, 2010, **2**, 461; (*b*) S. T. Zheng, J. Zhang, J. M. Clemente-Juan, D. Q. Yuan and G. Yang, *Angew. Chem., Int. Ed.*, 2009, **48**, 7176; (*c*) Z. M. Zhang, S. Yao, Y. G. Li, Y. H. Wang, Y. F. Qi and E. B. Wang, *Chem. Commun.*, 2008, 1650; (*d*) C. L. Hill, *J. Mol. Catal. A: Chem.*, 2007, **262**, 1–242; (*e*) A. Proust, R. Thouvenot and P. Gouzerh, *Chem. Commun.*, 2008, 1837.

11 (*a*) J. M. Clemente-Juan, E. Coronado and A. Gaita-Arino, *Chem. Soc. Rev.*, 2012, **41**, 7464; (*b*) C. Y. Sun, S. X. Liu, D. D. Liang, K. Z. Shao, Y. H. Ren and Z. M. Su, *J. Am. Chem. Soc.*, 2009, **131**, 1883; (*c*) X. Fang, P. Kögerler, Y. Furukawa, M. Speldrich and M. Luban, *Angew. Chem., Int. Ed.*, 2011, **50**, 5212; (*d*) S. Z. Li, J. W. Zhao, P. T. Ma, J. Du, J. Y. Niu and J. P. Wang, *Inorg. Chem.*, 2009, **48**, 9819; (*e*) S. T. Zheng, J. Zhang and G. Y. Yang, *Angew. Chem., Int. Ed.*, 2008, **47**, 3909; (*f*) M. Nyman, C. R. Powers, F. Bonhomme, T. M. Alam, E. J. Maginn and D. T. Hobbs, *Chem. Mater.*, 2008, **20**, 2513; (*g*) M. Ibrahim, M. H. Dickman, A. Suchopar and U. Kortz, *Inorg. Chem.*, 2009, **48**, 1649.

12 A.-X. Yan, S. Yao, Y.-G. Li, Z.-M. Zhang, Y. Lu, W.-L. Chen and E.-B. Wang, *Chem. – Eur. J.*, 2014, **20**, 6927.

13 (*a*) W.-C. Chen, X.-L. Wang, Y.-Q. Jiao, P. Huang, E.-L. Zhou, Z.-M. Su and K.-Z. Shao, *Inorg. Chem.*, 2014, **53**, 9486; (*b*) C. P. Pradeep, D.-L. Long, C. Streb and L. Cronin, *J. Am. Chem. Soc.*, 2008, **130**, 14946; (*c*) Y.-Q. Jiao, C. Qin, X.-L. Wang, C.-G. Wang, C.-Y. Sun, H.-N. Wang, K.-Z. Shao and Z.-M. Su, *Chem. – Asian J.*, 2014, **9**, 470.

14 D. Brown and D. Altermatt, *Acta Crystallogr., Sect. B: Struct. Sci.*, 1985, **41**, 244.

15 (*a*) A. L. Spek, *Acta Crystallogr., Sect. A: Found. Crystallogr.*, 1990, **46**, 194–201; (*b*) A. L. Spek, *PLATON99*, a Multipurpose Crystallographic Tool, Utrecht University, Utrecht, The Netherlands, 1999.

16 J.-S. Qin, S.-R. Zhang, D.-Y. Du, P. Shen, S.-J. Bao, Y.-Q. Lan and Z.-M. Su, *Chem. – Eur. J.*, 2014, **20**, 5625.

ESI

Supporting Information

Polyoxometalates-based Heterometallic Organic-Inorganic Hybrid Materials for Rapid Adsorption and Selective Separation of Methylene Blue from Aqueous Solution

Fei-Yan Yi,[a‡] Wei Zhu,[b‡] Song Dang,[a] Jian-Ping Li,[b] Dai Wu[b], Yun-hui Li[b] and Zhong-Ming Sun*[a]

[a]*State Key Laboratory of Rare Earth Resource Utilization, Changchun Institute of Applied Chemistry, Chinese Academy of Sciences, 5625 Renmin Street, Changchun, Jilin 130022, China. E-mail: szm@ciac.ac.cn*

[b]*School of Chemistry & Environmental Engineering, Changchun University of Science & Technology, Changchun 130022, China.*

Supplementary Index

1. Experimental Section

1.1. Materials and Methods

$K_8[\alpha\text{-}SiW_{11}O_{39}]\bullet 13H_2O$ was prepared according to the previous reports.[1] All other reagents and solvents were obtained from commercial sources without further purification.

Powder X-ray diffraction (PXRD) data were performed on a Rigaku/max 2550 diffractometer with Cu Kα radiation Field-emission (λ = 1.5418 Å, continuous, 40 kV, 40 mA, increment = 0.02°). The infrared (IR) spectra (diamond) were recorded on a Nicolet 7600 FT-IR spectrometer within the 4000-500 cm^{-1} region. TGA (thermal gravimetric analysis) was recorded under an air atmosphere with a heating rate of 10 °C/min using a a SDT 2960 Simultaneous DSC-TGA of TA instrument in the temperature range of 23-800 °C. UV−vis spectroscopic studies were collected on a UV-2450 spectrophotometer. The elemental analyses (EA) of C, H, N, S in the solid samples were carried out on a VarioEL analyzer (Elementar Analysensysteme GmbH). The metal Cu and K ions in the solution were analyzed via inductively coupled plasma (ICP) atomic emission spectrometric analysis (POEMS, TJA).

1.2 Syntheses of LnCu-POMs (1-4)

Compounds **1** and **4** were prepared by similar procedure. A mixture of $K_8[\alpha\text{-}SiW_{11}O_{39}]\bullet 13H_2O$ (150 mg), $CuCl_2\bullet 2H_2O$ (68 mg), $LnCl_3\bullet 6H_2O$ (90 mg) (Ln = Dy, **1**; Er, **4**) and en (**1**) or DETA (**4**) were dissolved in distilled water (10 mL) at room temperature. After stirring for 30 min, the suspension was placed into a 20 mL Teflon-lined stainless-steel container and heated at 150 °C for 5 days. After slow cooling to room temperature, blue-purple plate crystals were filtered, washed with distilled water, and dried in fume hood at room temperature to give a yield of 73% for **1** (based on W) $C_{16}H_{111}Cu_4Dy_2K_2N_{16}O_{101.5}Si_2W_{22}$ (*F*w = 6910.45): calcd. (%) C, 2.78; H, 1.62; N, 3.24; found (%) C, 2.59; H, 1.65; N, 3.21; and 60% for **4** (based on W) $C_{16}H_{77}CuErN_{12}O_{85}Si_2W_{22}$ (*F*w = 6129.58) calcd. (%) C, 3.14; H, 1.27; N, 2.74; found (%) C, 3.11; H, 1.50; N, 2.66. IR data (diamond, cm^{-1}) for **1**: 3441 (m), 3307 (s), 3253 (s), 2951 (w), 2891 (w), 1582 (s), 1458 (w), 1394 (w), 1367 (w), 1323 (w), 1281 (w), 1173 (w), 1097 (m), 1044 (m), 994 (m), 936 (m), 860 (m), 753 (m), 683 (m). IR data (diamond, cm^{-1}) for **4**: 3441 (m), 3307 (s), 3278 (s), 3140 (w), 2957 (w), 2891 (w), 2159 (w), 1582 (s), 1458 (m), 1394 (w), 1367 (w), 1323 (w), 1275 (m), 1167 (w), 1103 (m), 1038 (m), 994 (m), 942 (m), 876 (s), 757 (m), 671 (m).

When oxalic acid ($H_2C_2O_4$) was respectively added in the reaction mixtures used for **Dy-1** with en and **Dy-4** with DETA, blue-purple prism crystals of **Dy-2** and **Er-3** were obtained replacing **Dy-1** and **Er-4**, respectively. $C_{26}H_{126}Cu_6Er_2N_{24}O_{97}Si_2W_{22}$ (*F*w = 7144.15) calcd. (%) C, 4.37; H, 1.78; N, 4.71; found (%) C, 4.58; H, 1.49; N, 4.86. IR data (diamond, cm^{-1}) for **Dy-2**: 3550 (w), 3457 (m), 3307 (s), 3253 (s), 3146 (w), 2945 (w), 2881 (w), 2159 (w), 1653 (s), 1588 (s), 1458 (m), 1394 (w), 1361 (w), 1323 (w), 1275 (w), 1167 (w), 1097 (m), 1032 (m), 994 (m), 946 (m), 867 (s), 769

(m), 671 (m). IR data (diamond, cm^{-1}) for **Er-3**: 3550 (w), 3457 (m), 3302 (s), 3248 (s), 3146 (w), 3951 (w), 2887(w), 2159 (w), 1658 (m), 1576 (m), 1458 (m), 1399 (w), 1361 (w), 1319 (w), 1281 (w), 1173 (w), 1097 (w), 1038 (m),994 (m), 866 (s), 769 (m), 671 (m), 537 (w).

1.3 Dye absorption, separation and release

Dye absorption: Freshly prepared **Dy-1**, **Dy-2**, **Er-3** and **Er-4** samples with various qualities (1 mg, 2 mg, 5 mg, 8 mg and 10 mg) were trasferred into the aqueous solution of methylene blue (MB), methyl organge (MO), rhodamine-B (RhB) and Basic Red 2 (BR2) (20 mg/L) with 20 mL, respectively. After soaking for 24 h, the samples were separated through centrifuge to remove the suspended particle. Then the upper clear solutions were analyzed by a UV-vis spectrophotometer. Similarly, dye absorption for **1-4** towards aqueous solution of MB dye after given time intervals were prepared that freshly prepared **1-4** were dispersed in aqueous solution of MB (20 mL, 20 mg/L) for a regular interval time, then UV-vis spectra were also used to determine the adsorption of **1-4** after centrifuge.

Dye separation: Compounds **Dy-1**, **Dy-2**, **Er-3** and **Er-4** were transferred into the mixtures (20 mL) of MB and RhB, MB and MO (*v*:*v* 1/1, 20 mg/L), respectively. At given time intervals, UV-vis spectra were measured to analysis the selective adsorption ability of **1-4**.

Dye release: the **Dy-1**, **Dy-2**, **Er-3** and **Er-4** loaded with MB were activated with a mixed solvent EtOH/H_2O (*v*:*v* 1:1) of NaCl at room temperature, respectively. The regenerated **Dy-1** sample was dried overnight at 80 °C and reused for the next adsorption. The MB solution from MB@Dy-1 in other various solutions have also been used to monitor the release process in UV-vis spectra, such as pure water, pure ethanol solvent, the aqueous solution of NaCl, as well as the mixed solvents of NaCl with ethanol and water for different volume ratio (1:9 and 9:1).

1.4 Single Crystal X-ray structure determination

Single crystals of **1**, **3** and **4** were selected for indexing and data collection on a Bruker Apex II CCD diffractometer with graphite monochromated Mo-K*a* radiation (λ = 0.71073 Å) at 296 K. Data processing was accomplished with the SAINT program. All absorption corrections were applied using the multi-scan program SADABS.[2] All structures were solved by direct methods using SHELXS-97 program of the SHELXTL package and refined by the full-matrix least squares method with SHELXTL-97.[3] All non-hydrogen atoms were easily found from the difference Fourier map and refined using the full-matrix least-squares method on F^2 with anisotropic thermal parameters during the final cycles except of some disordered oxygen and carbon atoms, as follows. The positions of the hydrogen atoms attached to the carbon and nitrogen atoms were refined isotropically as a riding mode. The hydrogen atoms attached to water molecules were not located in all compounds and just put into the final molecular formula. The occupancy factors of O(48), O(3W) and O(15W) in **Dy-1** as well as O(9W) and O(10W) in **Er-4** were reduced to 50% because

of their large thermal parameters. The program SQUEEZE in PLATON was used to calculate the solvent area and remove their contribution to the overall intensity data in **Dy-1** and **Er-4**. See the CIF file for details. Crystallographic data for **1**, **3** and **4** is summarized in Table S1. Selected bond distances are given in Table S3. The BVS values of all Er, W and O atoms except the lattice water molecules in **Er-4** are listed in Table S2.

Because most of POMs-structures are larger than simple coordination complexes and there are a large amount of weight atoms in their structures, it is very difficult to refine these large structures. Moreover, the quality of crystals are not very good, which usually leads to the case that the quality of intensity data is not perfect, as a result, some atoms have the ADP max/min ratios. Therefore, some disordered atoms have been isotropically refined.

1: The ISOR instruction is used for C1, C2, N8, O17, O22, O23, O36, O38, O48, O58, O29, and O11W.

3: The ISOR instruction is used for Si1, C2, O8, O20, O26, O67, O76, and O6W.

4: The ISOR instruction is used for O53.

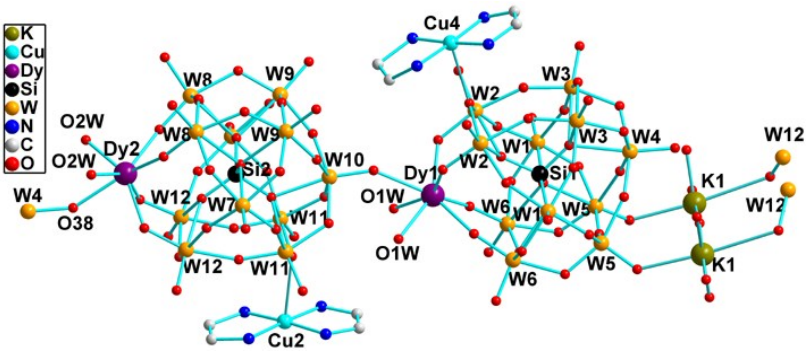

(a)

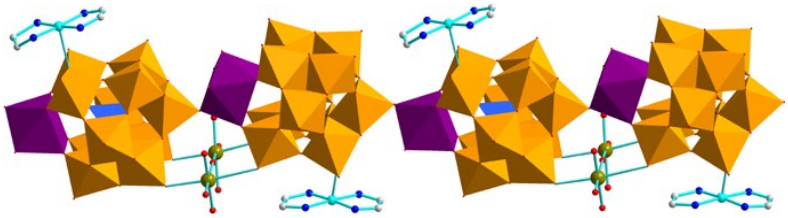

(b)

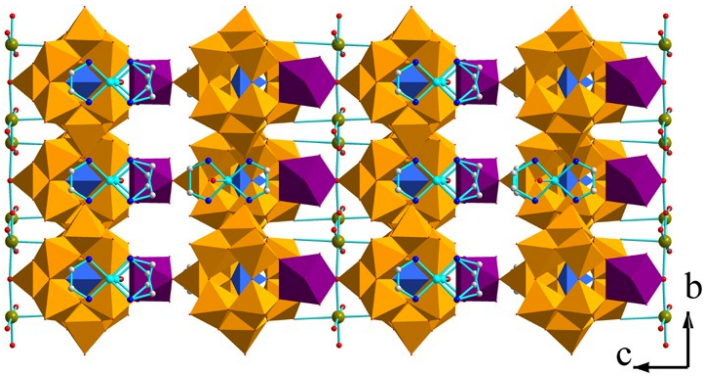

(c)

Fig. S1 (a) Representation of the molecular structure unit of **Dy-1**. The hydrogen atoms, discrete $[Cu(H_2O)(en)_2]^{2+}$ ions, and crystal water molecules are omitted for clarity. (b) The polyhedral view of 1D chain LnCu-POMs of **Dy-1**. (c) The 3D supramolecular architecture along the [100] direction. WO_6 octahedra, gold; SiO_4 tetrahedra, blue; DyO_7 polyhedra, purple; K, dark yellow sphere; C, grey sphere; N, dark blue spheres.

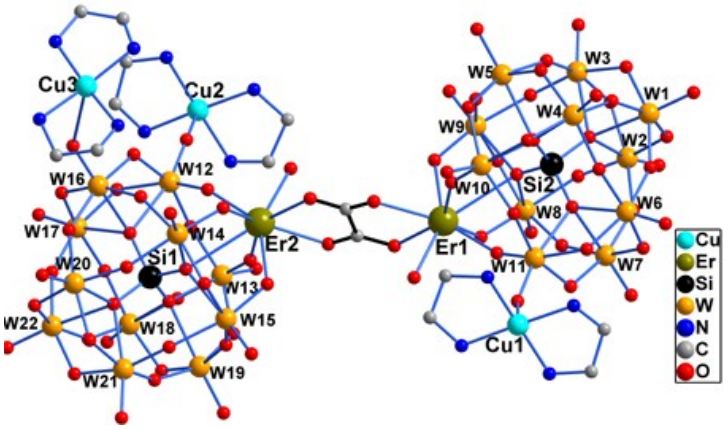

Fig. S2 Representation of the molecular structure unit of **Er-3 (Dy-2)**. The hydrogen atoms, discrete $[Cu(H_2O)(en)_2]^{2+}$ ions, and crystal water molecules are omitted for clarity.

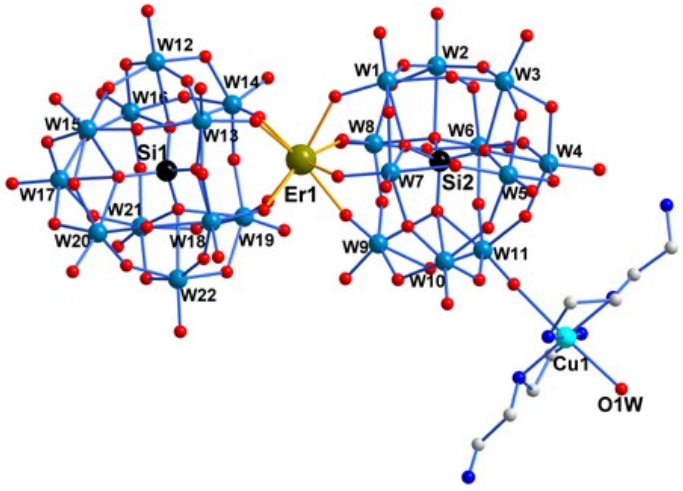

(a)

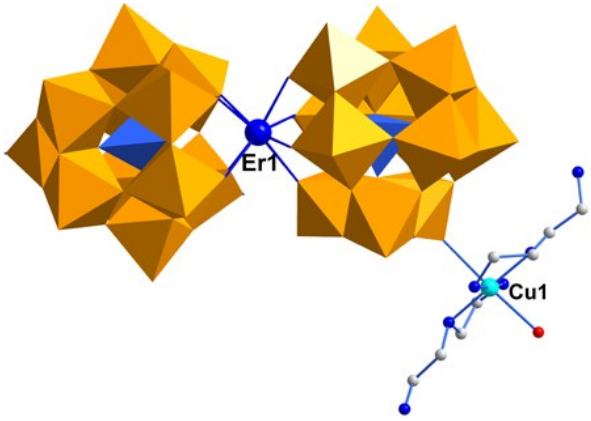

(b)

Fig. S3 (a) Representation of the molecular structure unit of **Er-4**. The hydrogen atoms, DETA

molecules, and crystal water molecules are omitted for clarity. (b) The polyhedral view of the dimer of **Er-4**.

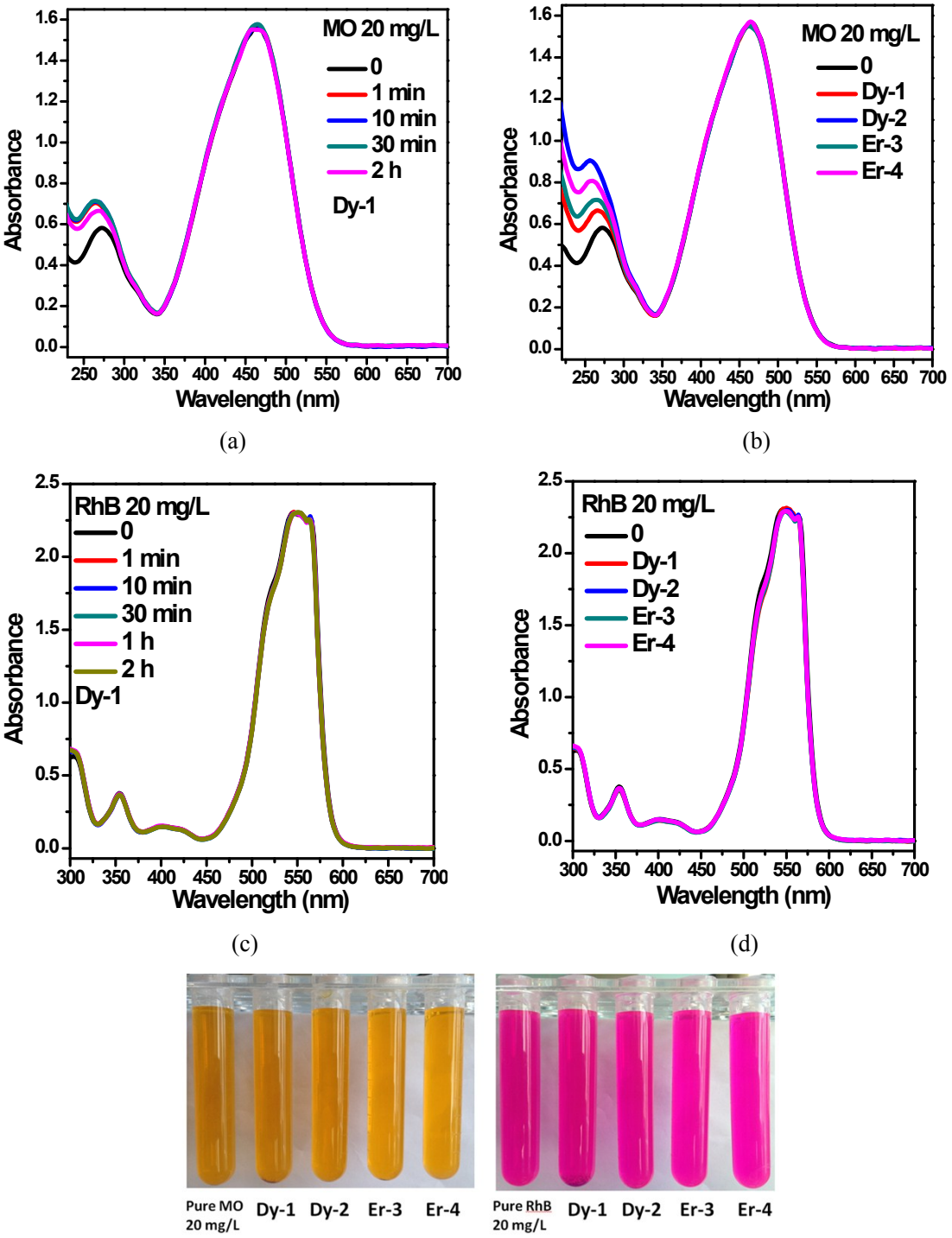

Fig. S4 UV-vis spectra and photographs of aqueous solution of MO (20 mg/L) and RhB (20 mg/L) dyes with **Dy-1** after immersing different time (a and c), as well as with **Dy-1**, **Dy-2**, **Er-3** and **Er-4** (5 mg) after immersing for 24 h.

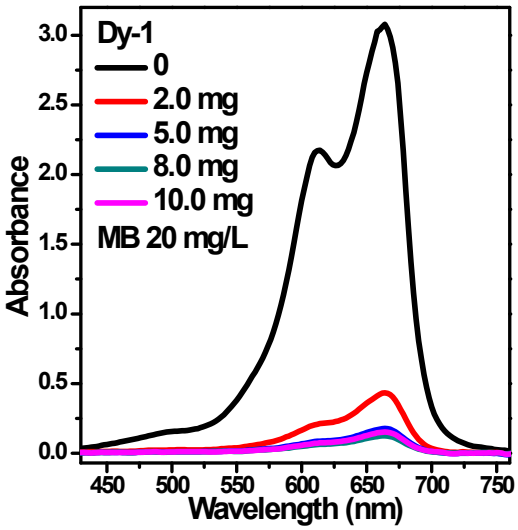
Dy-1
0
2.0 mg
5.0 mg
8.0 mg
10.0 mg
MB 20 mg/L
Absorbance
Wavelength (nm)

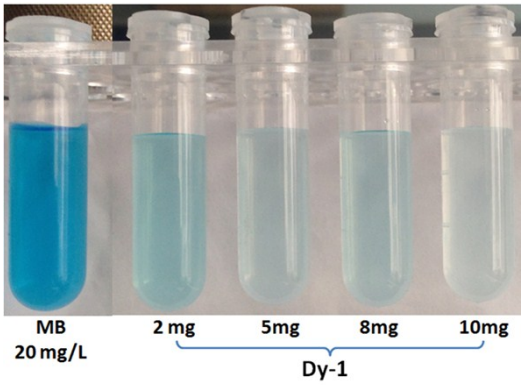
MB
20 mg/L
2 mg
5mg
8mg
10mg
Dy-1

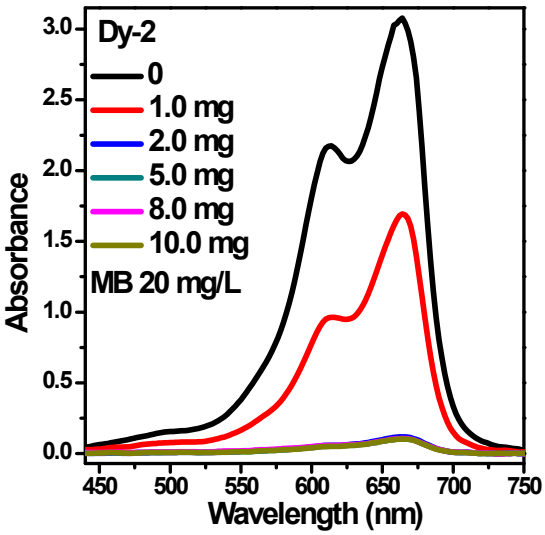
Dy-2
0
1.0 mg
2.0 mg
5.0 mg
8.0 mg
10.0 mg
MB 20 mg/L
Absorbance
Wavelength (nm)

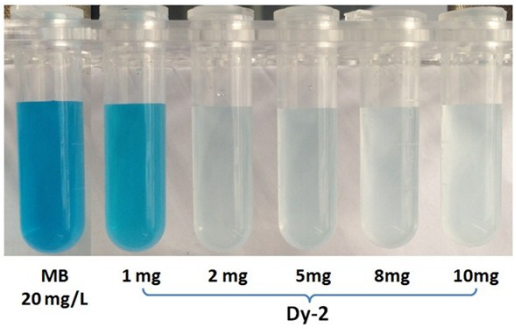
MB
20 mg/L
1 mg
2 mg
5mg
8mg
10mg
Dy-2

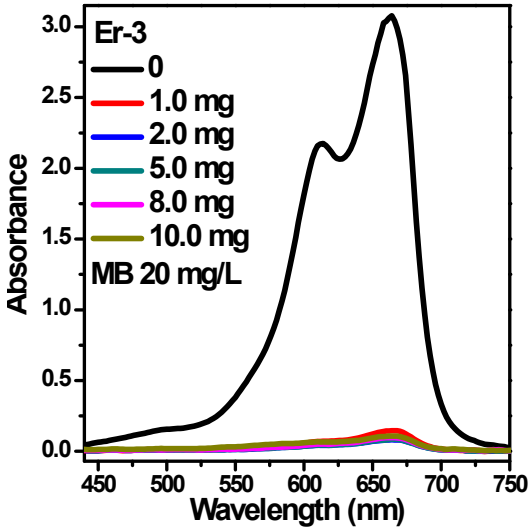
Er-3
0
1.0 mg
2.0 mg
5.0 mg
8.0 mg
10.0 mg
MB 20 mg/L
Absorbance
Wavelength (nm)

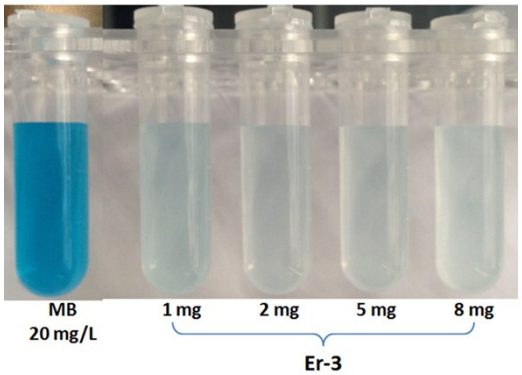
MB
20 mg/L
1 mg
2 mg
5 mg
8 mg
Er-3

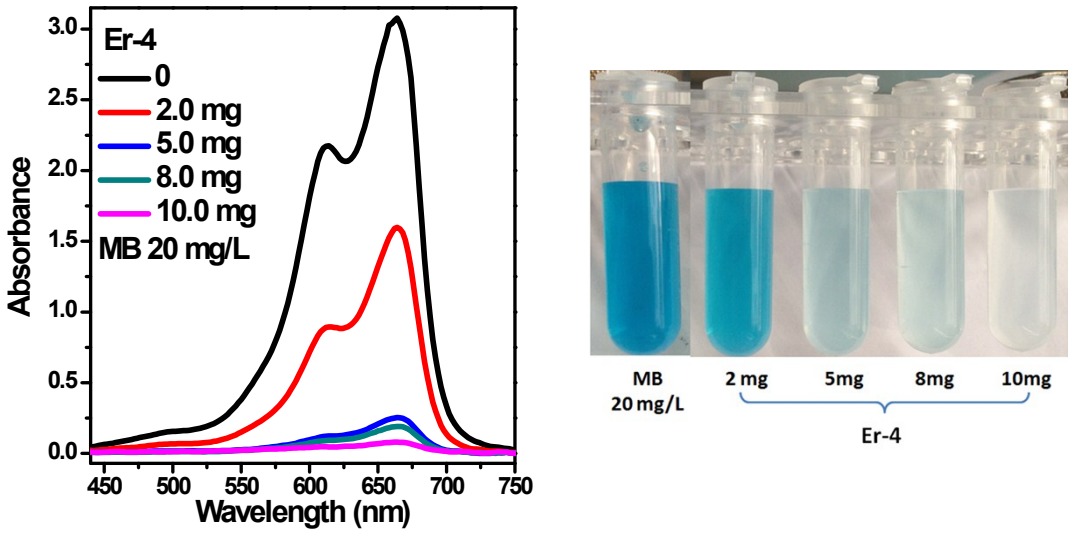

Fig. S5 **Dy-1**, **Dy-2**, **Er-3** and **Er-4** were used to adsorb MB (20 mg/L, 20 mL) in aqueous solution with different quality (mg), as well as the related contrastive photographs of dye solutions before (MB, 20 mg/L) and after with different quality of **1-4**.

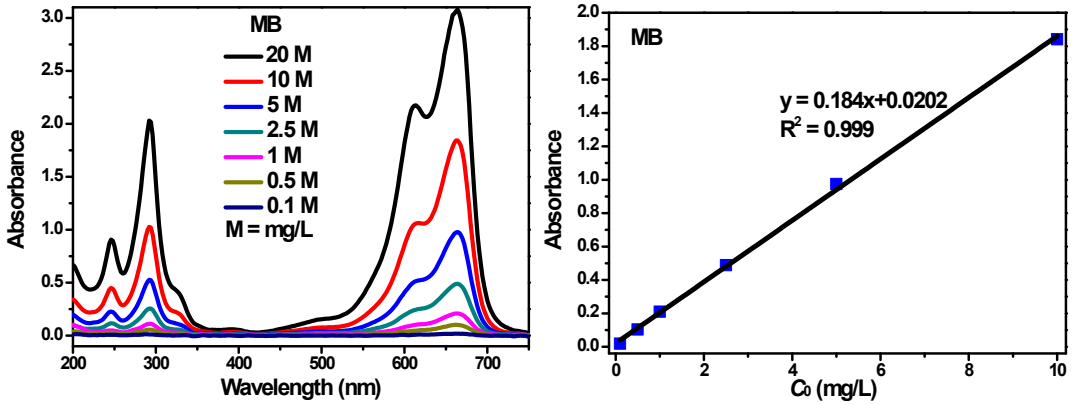

Fig. S6 (a) UV-vis spectra of aqueous solutions of MB dye with different concentrations. (b) The absorbed intensity (blue dots) of MB dye in different concentrations (C_0 = mg/L). The black solid line is the best linear fit.

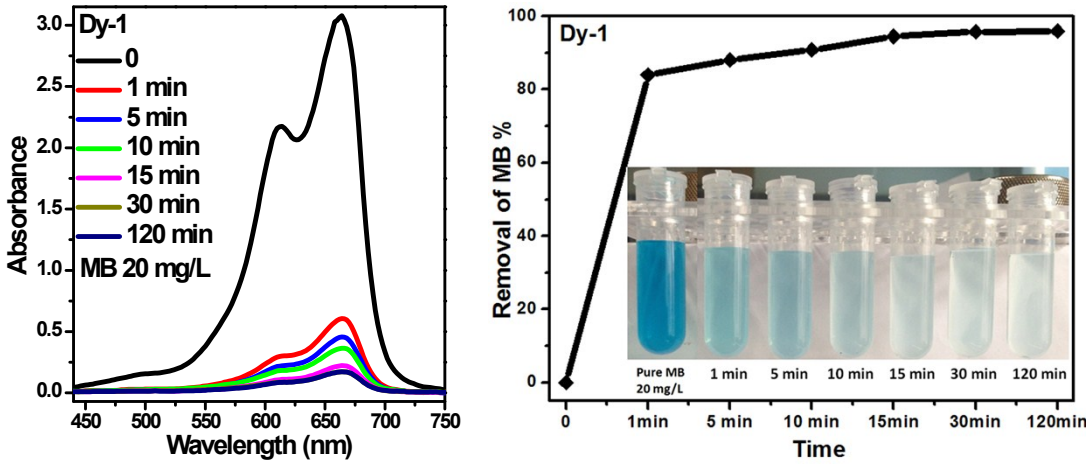

(a) (b)

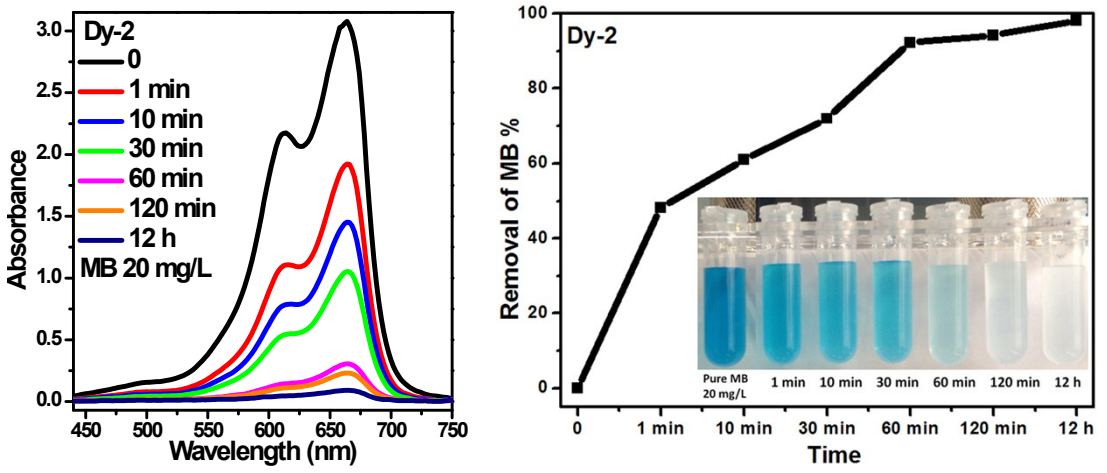

(c) (d)

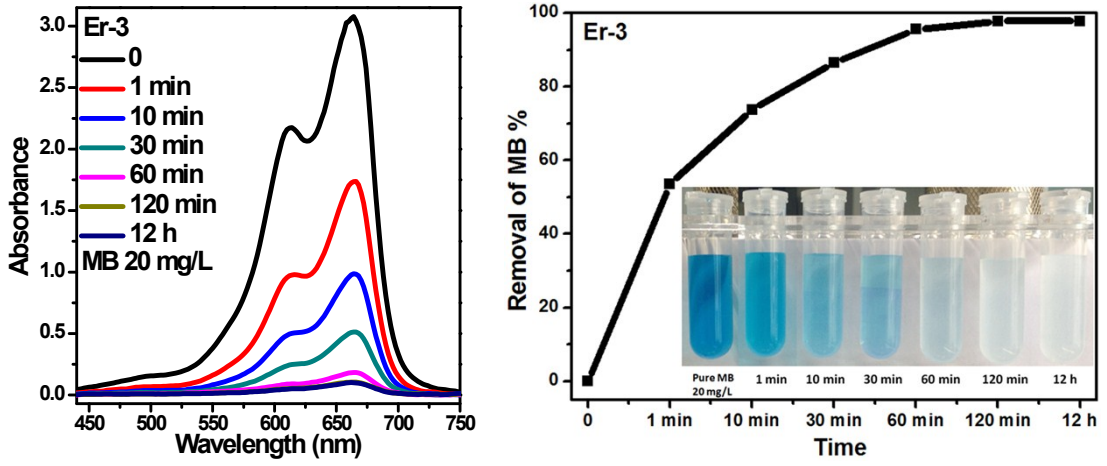

(e) (f)

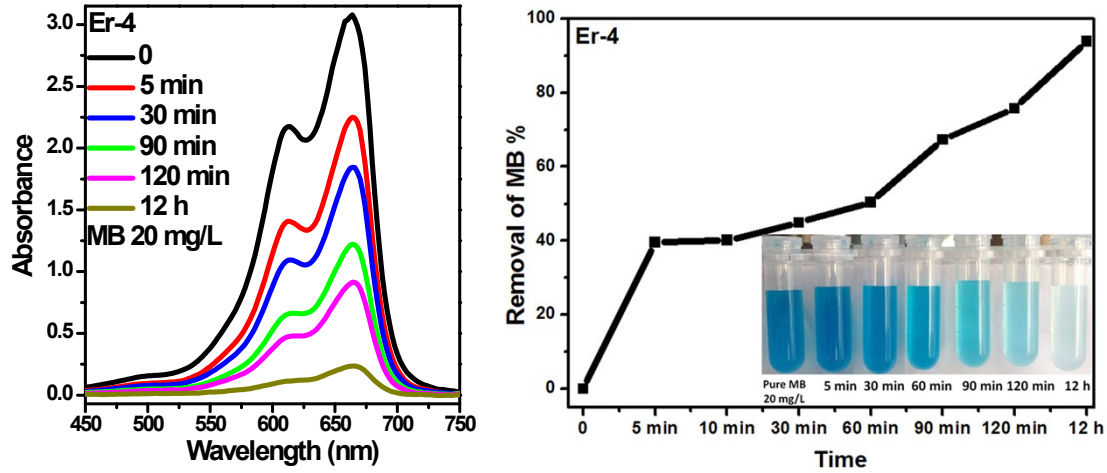

(g) (h)

Fig. S7 (a, c, e and g) The UV-vis spectra of the adsorption rate with **Dy-1**, **Dy-2**, **Er-3** and **Er-4** (5.0 mg) towards MB (20 mg/L, 20 mL). (b, d, f and h) The corresponding removal efficiency on the MB dye for **1-4**. Insert: the comparative photographs after different adsorbed time.

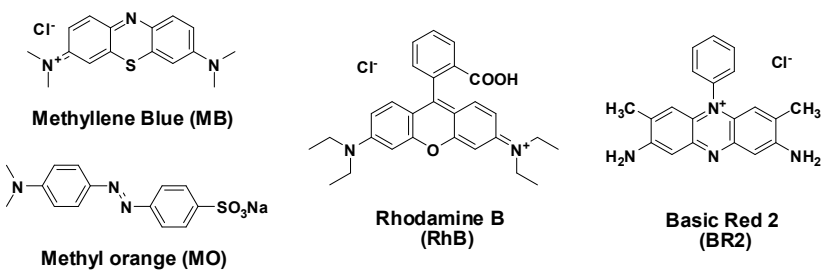

Fig. S8 The structures of dyes, MB, MO, RhB, and BR2.

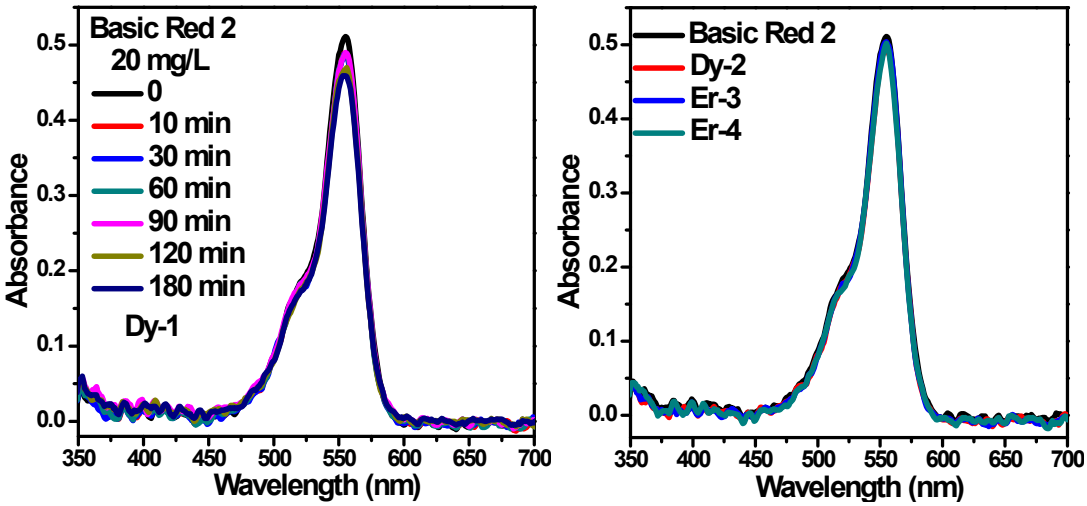

Fig. S9 UV-vis spectra of aqueous solution of BR2 (20 mg/L) dye with **Dy-1** (5 mg) after immersing different time, as well as with **Dy-2**, **Er-3** and **Er-4** (5 mg) after immersing for 24 h.

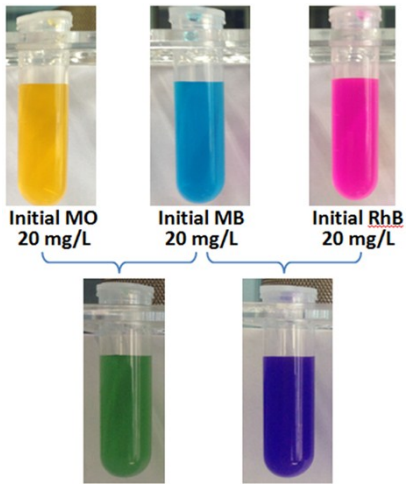

(a)

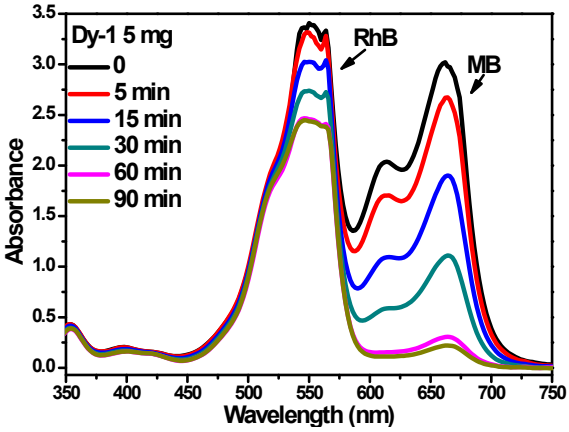
Dy-1 5 mg
0
5 min
15 min
30 min
60 min
90 min
RhB
MB
Absorbance
Wavelength (nm)

(b)

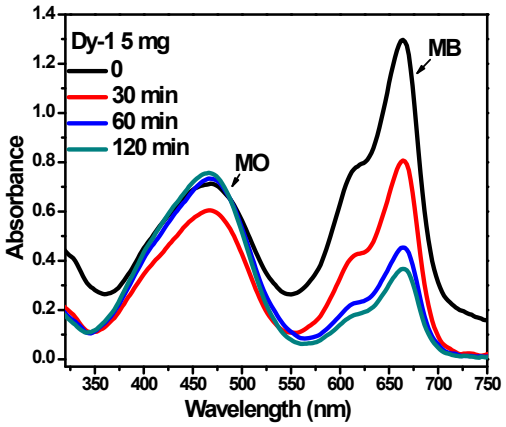
Dy-1 5 mg
0
30 min
60 min
120 min
MO
MB
Absorbance
Wavelength (nm)

(c)

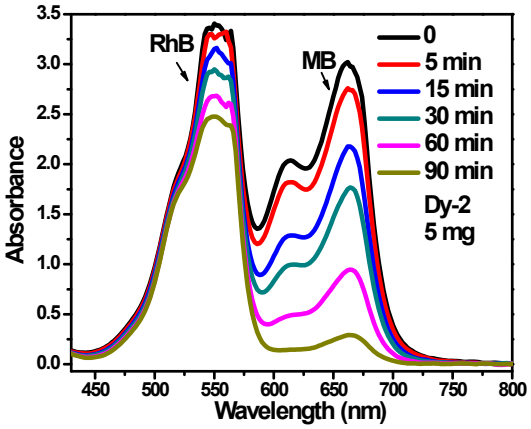
RhB
MB
0
5 min
15 min
30 min
60 min
90 min
Dy-2
5 mg
Absorbance
Wavelength (nm)

(d)

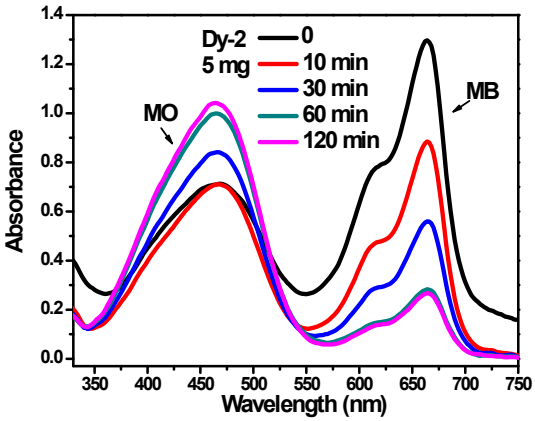
Dy-2
5 mg
0
10 min
30 min
60 min
120 min
MO
MB
Absorbance
Wavelength (nm)

(e)

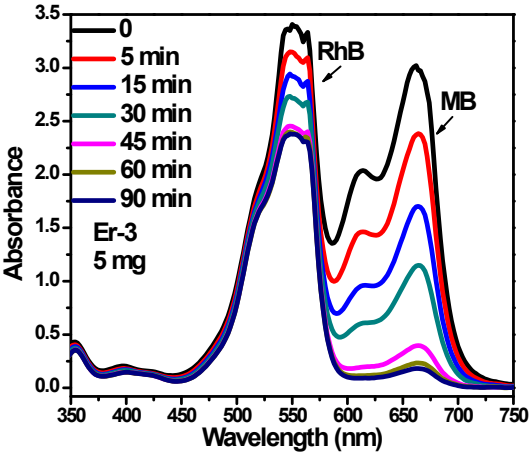
0
5 min
15 min
30 min
45 min
60 min
90 min
Er-3
5 mg
RhB
MB
Absorbance
Wavelength (nm)

(f)

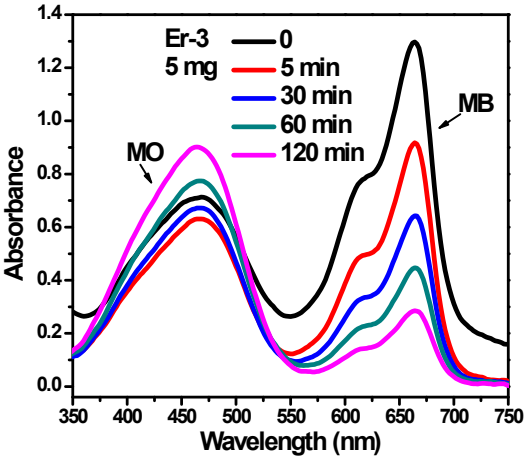
Er-3
5 mg
0
5 min
30 min
60 min
120 min
MO
MB
Absorbance
Wavelength (nm)

(g)

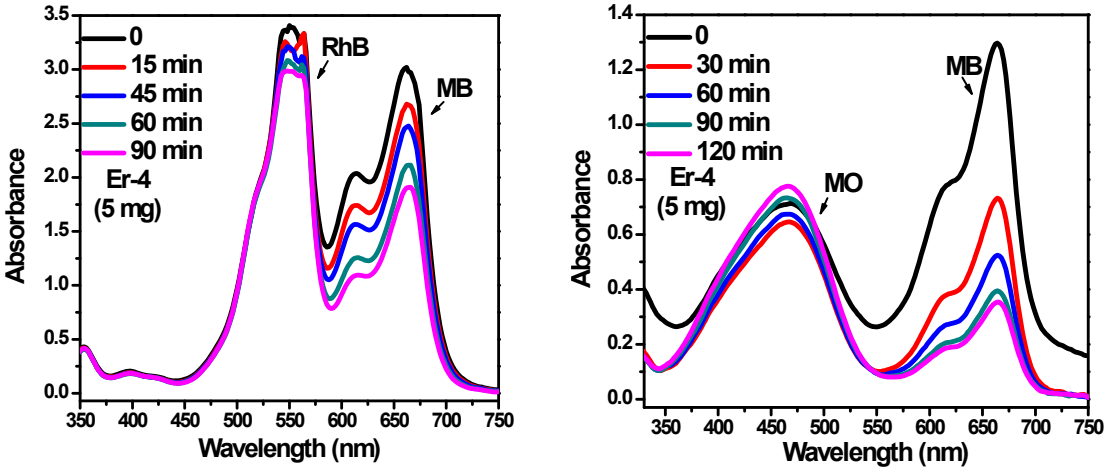

(h) (i)

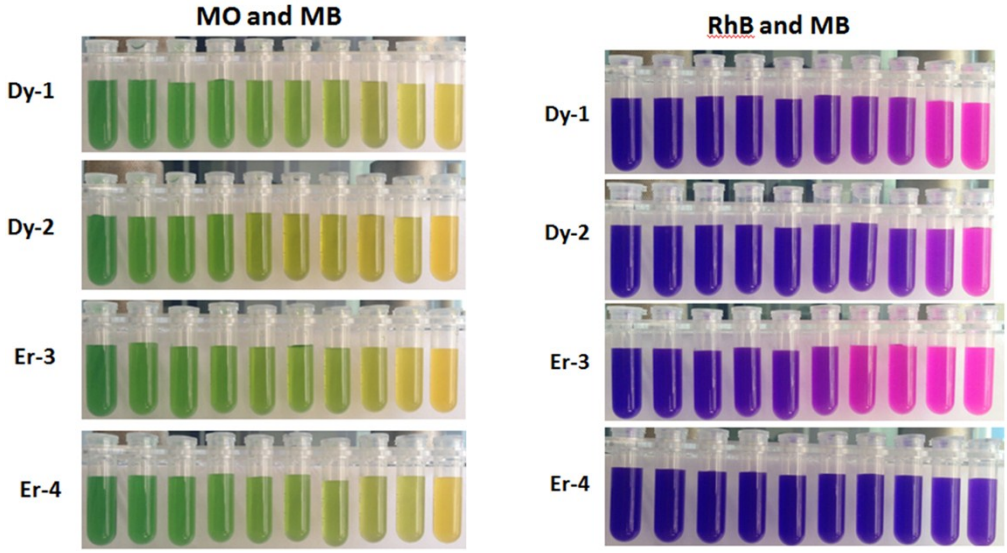

(j) (k)

Fig. S10 (a) The photographs of initial MB, MO and RhB solution, as well as the mixed dye solutions of MB and MO, MB and RhB. (b-i) UV-vis spectra of aqueous solution of dyes with **Dy-1** (b and c), **Dy-2** (d and e), **Er-3** (f and g) and **Er-4** (h and i). (b, d, f and h) RhB and MB. (c, e, g and i) MO and MB. (j and k) Photographs of dye selective adsorption of **Dy-1**, **Dy-2**, **Er-3** and **Er-4**.

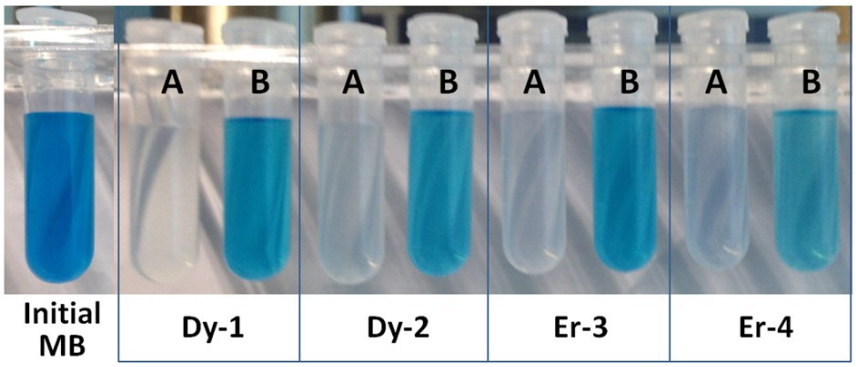

Fig. S11 The contrastive photographs of MB dye solution after adsorption-desorption process for

Dy-1, **Dy-2**, **Er-3** and **Er-4**. A: The solution of MB dye after adsorption with different compounds **1-4**; B: The solution of MB from MB@**Dy-1** (**Dy-2**, **Er-3** and **Er-4**) in ethanol solution of NaCl.

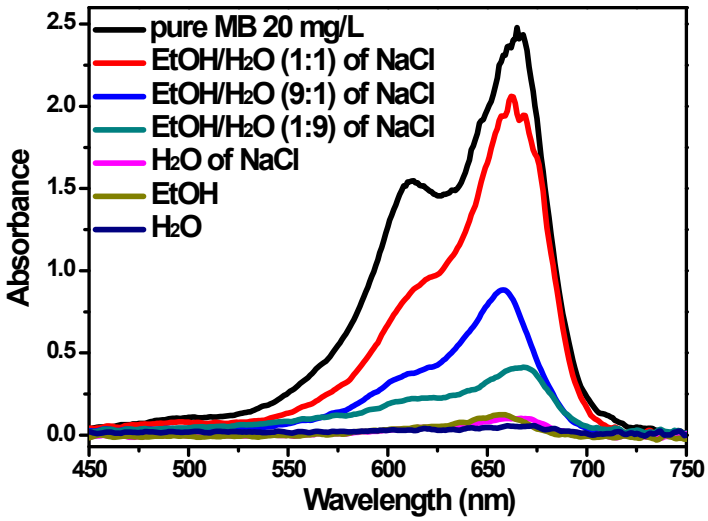

Fig. S12 The UV-vis spectra of desorbed MB solution from MB@Dy-1 using various elution solutions, such as, pure aqueous solution (H_2O), pure ethanol solvent (EtOH), the aqueous solution of NaCl (H_2O of NaCl), the mixed solvents with EtOH and H_2O of NaCl for different volume ratio (EtOH/H_2O (1:1) of NaCl, EtOH/H_2O (9:1) of NaCl, EtOH/H_2O (1:9) of NaCl).

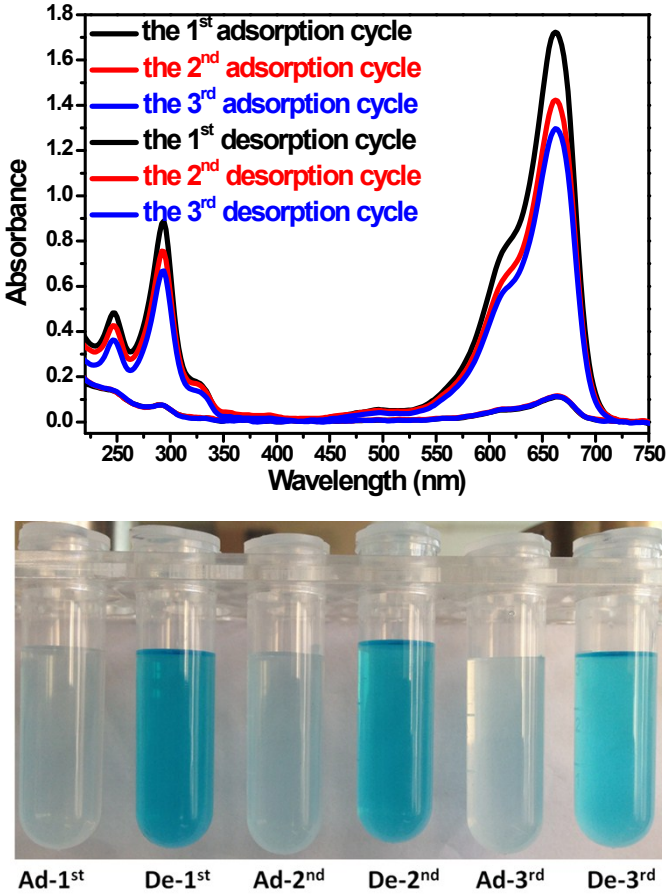

Fig. S13 The UV-vis spectra and photographs of three adsorption and desorption cycles for **Dy-1**,

the first cycle: Ad-1st and De-1st; the second cycle: Ad-2nd and De-2nd; the third cycle: Ad-3rd and De-3rd.

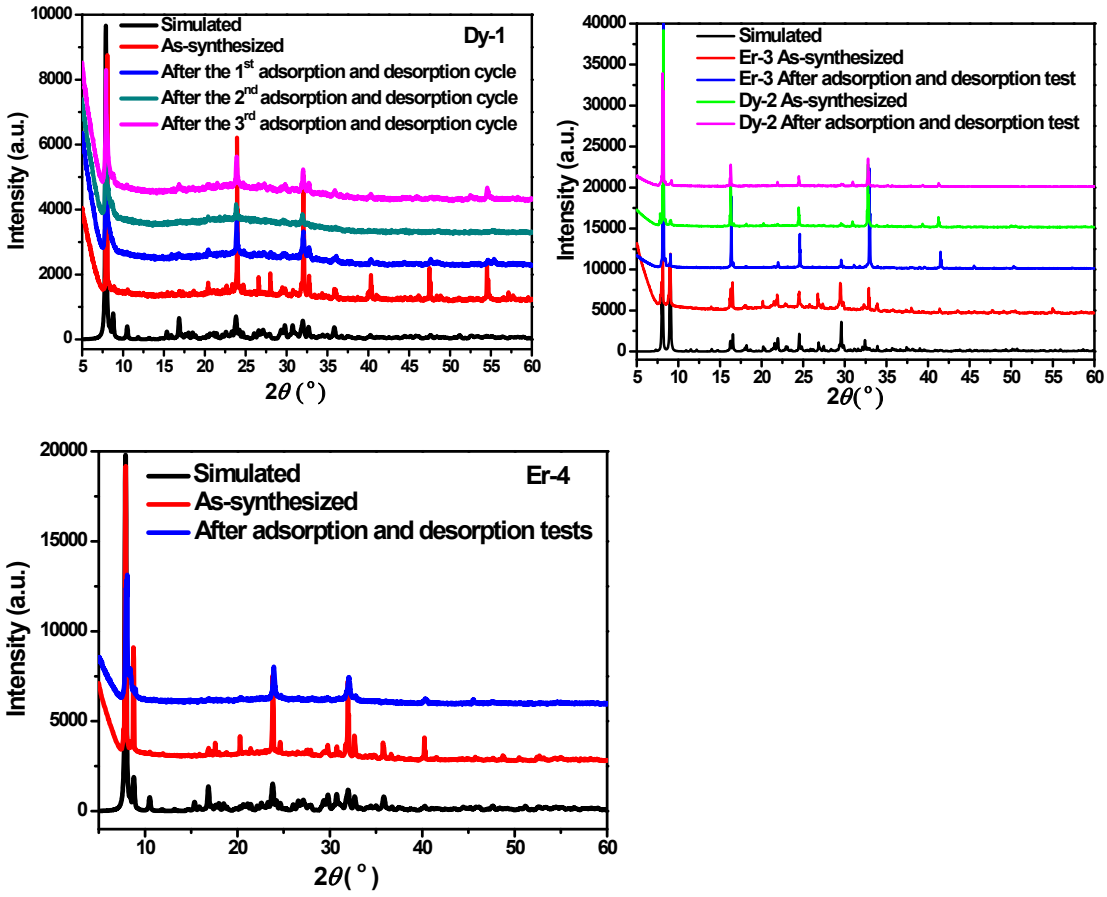

Fig.S14 PXRD patterns for **Dy-1**, **Dy-2**, **Er-3** and **Er-4**.

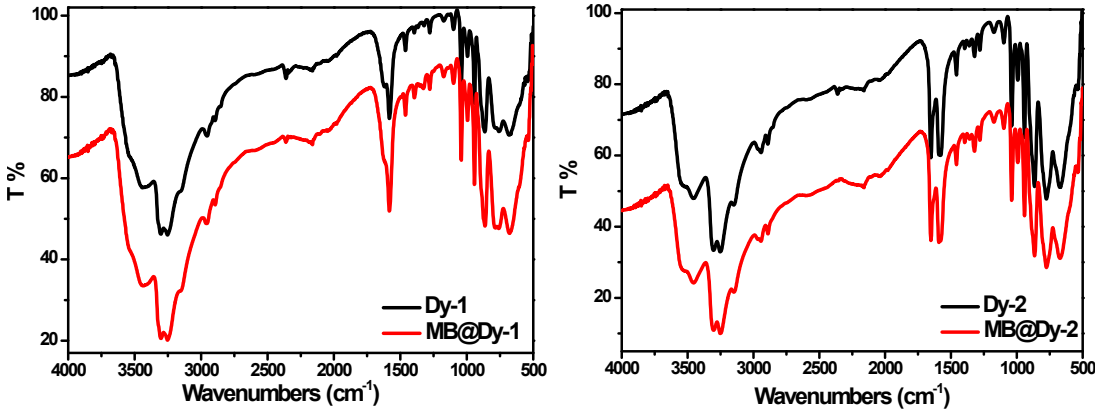

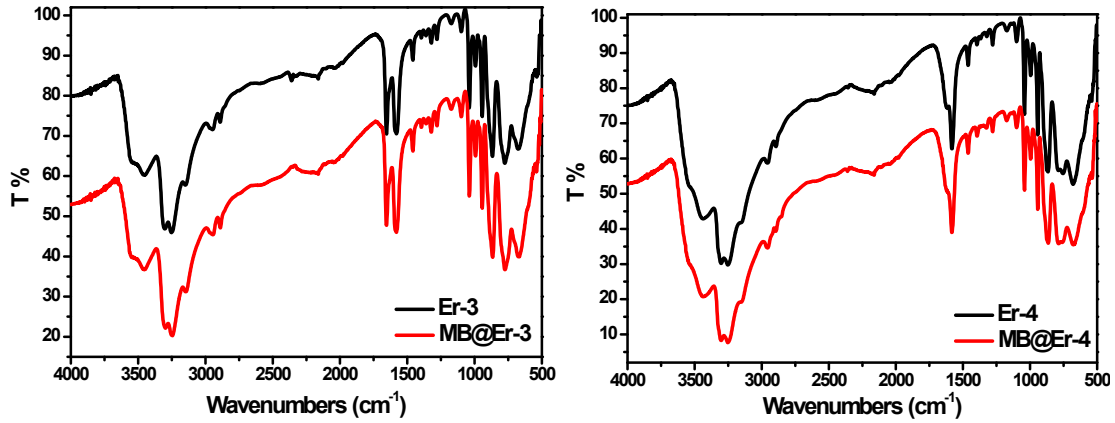

Fig. S15 FT-IR spectra for **Dy-1**, **Dy-2**, **Er-3** and **Er-4**, as well as the related MB@LnCu-POMs (**1-4**).

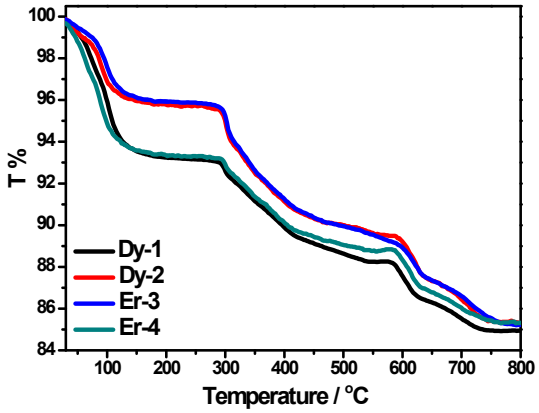

Fig. S16 TGA curves of **Dy-1**, **Dy-2**, **Er-3** and **Er-4**.

The TG curves of compounds **1-4** show three weight loss steps. The first weight loss corresponds to the releases of free and coordinated water molecules (for **Dy-1**: found. 6.50%, calcd. 6.24%; for **Er-3**: found. 3.88%, calcd. 3.28%; for **Er-4**: found. 6.32%, calcd. 5.13%) in the range from room temperature to 153 °C. The total weight loss at 750 °C is 15.1% for **Dy-1**, 14.6% for **Dy-2,** 14.73% for **Er-3**, 14.66% for **Er-4**.

Table S1 Summary of Crystal Data and Structure Results for 1-4.

Compound	**Dy-1**	**Er-3**	**Er-4**
CCDC	1028827	1028828	1028829
Empirical formula	$C_{16}H_{111}Cu_4Dy_2K_2N_{16}O_{101.5}Si_2W_{22}$	$C_{26}H_{126}Cu_6Er_2N_{24}O_{97}Si_2W_{22}$	$C_{16}H_{77}CuErN_{12}O_{85}Si_2W_{22}$
structural formula#	$[K_2(H_2O)_{6.5}][Cu(en)_2]_2[Dy(H_2O)_2SiW_{11}O_{39}]_2$•2$[Cu(H_2O)(en)_2]$•10$H_2O$	$[Cu(en)_2]_3[Er(H_2O)SiW_{11}O_{39}]_2(C_2O_4)$•$[Cu(H_2O)(en)_2]_3$•10$H_2O$	$[Cu(H_2O)(DETA)_2]H_{11}[Er(SiW_{11}O_{39})_2]$•2DETA•6$H_2O$
fw	6910.45	7144.15	6129.58

Crystal system	Monoclinic	Orthorhombic	Monoclinic
Space group	*C*m	*F*dd2	$P2_1c$
Temperature (K)	296(2)	296(2)	296(2)
λ (Mo Kα), Å	0.71073	0.71073	0.71073
a /Å	20.5847(11)	43.425(3)	19.142(6)
b /Å	13.4613(7)	43.548(3)	24.362(7)
c /Å	22.9069(13)	25.625(2)	21.693(6)
α /°	90	90	90
β /°	101.9730(10)	90	99.006(7)
γ /°	90	90	90
V /Å^3	6209.3(6)	48461(6)	9992(5)
Z	2	16	4
2θ max (deg)	52.18	52.22	52.12
μ(Mo-Kα) mm^{-1}	22.331	23.320	26.379
D, g/cm^3	3.696	3.917	4.075
F(000)	6146	51072	10760
Crystal size (mm^3)	0.42 × 0.31 × 0.27	0.31 × 0.30 × 0.25	0.36 × 0.31 × 0.17
Reflections collected / unique	19627/8892 [R_{int} = 0.0450]	75181/23546[R_{int} = 0.0792]	59396/19612 [R_{int} = 0.0774]
Final *R* indices [$I > 2\sigma(I)$]	$^aR_1$ = 0.0407, $^bwR_2$ = 0.0970	$^aR_1$ = 0.0468, $^bwR_2$ = 0.1039	$^aR_1$ = 0.0461, $^bwR_2$ = 0.0997
R indices (all data)	$^aR_1$ = 0.0497, $^bwR_2$ = 0.1028	$^aR_1$ = 0.0647, $^bwR_2$ = 0.1139	$^aR_1$ = 0.0707, $^bwR_2$ = 0.1077
GOF	1.067	1.028	1.022

$^a R_1 = \sum||F_o| - |F_c||/\sum|F_o|$, $^b wR_2 = \{\sum w[(F_o)^2-(F_c)^2]^2/\sum w[(F_o)^2]^2\}^{1/2}$

#: These formulas were determined by considering crystal structures and other analyses (EA, TGA, and BVS) together.

Table S2. The BVS values of all the atoms except the lattice water molecules in **Er-4**.

Atoms	BVS values	Atoms	BVS values
Er1	2.89	Si1	3.87
Si2	3.98	W1	6.13
W2	6.16	W3	6.25
W4	6.22	W5	6.18

W6	6.26	W7	5.92
W8	5.94	W9	6.17
W10	6.19	W11	6.10
W12	6.11	W13	5.88
W14	6.25	W15	5.90
W16	6.14	W17	6.22
W18	5.94	W19	5.88
W20	6.04	W21	5.97
W22	6.04		
O1	1.71	O2	1.90
O3	1.97	O4	1.89
O5	1.60	O6	1.83
O7	1.76	O8	1.98
O9	1.75	O10	1.78
O11	1.65	O12	2.08
O13	1.85	O14	1.91
O15	1.98	O16	1.91
O17	1.65	O18	1.85
O19	1.86	O20	2.02
O21	1.95	O22	1.94
O23	1.89	O24	2.08
O25	1.88	O26	1.70
O27	2.03	O28	1.93
O29	1.87	O30	1.93
O31	1.92	O32	2.02
O33	2.00	O34	1.89
O35	1.90	O37	1.90
O38	1.70	O39	1.78
O42	1.74	O43	1.67
O44	1.90	O45	1.67
O46	1.54	O47	1.70
O48	1.83	O49	1.92
O50	1.92	O51	2.07
O52	2.04	O53	1.84
O54	1.94	O55	1.76
O56	2.06	O57	1.99
O58	1.60	O59	1.82
O60	1.81	O66	1.81
O67	1.93	O68	1.86
O69	1.74	O70	1.94
O71	1.73	O72	1.80
O73	1.89	O74	1.82
O75	1.98	O76	1.87

O77	1.87	O78	2.08
O79	2.03	O80	1.91
O81	1.83	O91	1.88
O92	1.60	O93	1.57
O94	1.77	O95	1.54

Table S3. Selected bond lengths for **1**, **3** and **4**.

Compound Dy-1			
Cu(1)-N(6)	1.96(3)	Cu(1)-N(5)#2	2.00(2)
Cu(1)-N(6)#2	1.96(3)	Cu(1)-N(5)	2.00(2)
Cu(2)-N(2)	1.98(3)	Cu(2)-N(1)	2.01(3)
Cu(2)-N(2)#2	1.98(3)	Cu(2)-N(1)#2	2.01(3)
Cu(3)-N(8)#2	2.02(3)	Cu(3)-N(7)	2.04(3)
Cu(3)-N(8)	2.02(3)	Cu(3)-N(7)#2	2.04(3)
Cu(3)-O(8W)	2.43(4)	Cu(4)-N(3)	1.92(3)
Cu(4)-N(3)#2	1.92(3)	Cu(4)-N(4)	1.97(3)
Cu(4)-N(4)#2	1.97(3)	Dy(1)-O(7)	2.276(16)
Dy(1)-O(9)#2	2.253(15)	Dy(1)-O(1W)#2	2.360(15)
Dy(1)-O(9)	2.253(15)	Dy(1)-O(1W)	2.360(15)
Dy(1)-O(7)#2	2.276(16)	Dy(1)-O(6)	2.48(2)
Dy(2)-O(44)#2	2.291(16)	Dy(2)-O(2W)	2.35(2)
Dy(2)-O(44)	2.291(16)	Dy(2)-O(2W)#2	2.35(2)
Dy(2)-O(26)#2	2.299(16)	Dy(2)-O(38)#3	2.411(19)
Dy(2)-O(26)	2.299(17)	Dy(2)-O(3W)	2.54(6)
Si(1)-O(11)	1.61(2)	Si(1)-O(12)#2	1.614(16)
Si(1)-O(12)	1.614(16)	Si(1)-O(10)	1.66(2)
Si(2)-O(31)	1.634(16)	Si(2)-O(41)	1.64(2)
Si(2)-O(31)#2	1.634(16)	Si(2)-O(5)	1.65(2)
W(1)-O(14)	1.709(17)	W(1)-O(35)	1.932(16)
W(1)-O(17)#2	1.850(17)	W(1)-O(32)	1.935(16)
W(1)-O(13)	1.870(17)	W(1)-O(12)	2.331(14)
W(2)-O(37)	1.745(16)	W(2)-O(36)	1.970(13)
W(2)-O(9)	1.808(14)	W(2)-O(21)	2.031(15)
W(2)-O(35)	1.897(16)	W(2)-O(10)	2.246(15)
W(3)-O(19)	1.704(18)	W(3)-O(20)	1.922(10)
W(3)-O(21)	1.864(16)	W(3)-O(15)	1.945(14)
W(3)-O(32)	1.894(17)	W(3)-O(11)	2.387(16)
W(4)-O(38)	1.710(19)	W(4)-O(15)	1.906(15)
W(4)-O(16)	1.877(16)	W(4)-O(15)#2	1.906(15)
W(4)-O(16)#2	1.877(16)	W(4)-O(11)	2.32(2)
W(5)-O(39)	1.702(17)	W(5)-O(16)#2	1.965(15)
W(5)-O(8)	1.811(15)	W(5)-O(17)	1.967(18)

W(5)-O(18)	1.900(4)	W(5)-O(12)#2	2.413(16)
W(6)-O(40)	1.700(19)	W(6)-O(13)#2	2.02(2)
W(6)-O(7)	1.788(18)	W(6)-O(8)	2.026(18)
W(6)-O(47)	1.896(8)	W(6)-O(12)#2	2.338(14)
W(7)-O(28)	1.683(17)	W(7)-O(27)	1.945(17)
W(7)-O(43)	1.850(15)	W(7)-O(30)	1.998(18)
W(7)-O(29)	1.886(14)	W(7)-O(31)	2.315(14)
W(8)-O(26)	1.727(17)	W(8)-O(27)	1.960(18)
W(8)-O(25)	1.757(16)	W(8)-O(23)	2.039(15)
W(8)-O(24)	1.927(8)	W(8)-O(31)	2.374(15)
W(9)-O(34)	1.683(17)	W(9)-O(22)	1.911(5)
W(9)-O(23)	1.851(17)	W(9)-O(33)	1.923(16)
W(9)-O(30)	1.855(19)	W(9)-O(31)	2.335(15)
W(10)-O(6)	1.690(19)	W(10)-O(4)#2	1.92(2)
W(10)-O(33)#2	1.914(16)	W(10)-O(4)	1.92(2)
W(10)-O(33)	1.914(16)	W(10)-O(5)	2.331(18)
W(11)-O(2)	1.704(15)	W(11)-O(4)	1.95(2)
W(11)-O(3)	1.800(17)	W(11)-O(29)#2	1.958(14)
W(11)-O(1)	1.917(11)	W(11)-O(5)	2.338(15)
W(12)-O(46)	1.680(15)	W(12)-O(43)#2	1.983(17)
W(12)-O(44)	1.793(16)	W(12)-O(3)	2.067(18)
W(12)-O(45)	1.920(11)	W(12)-O(41)	2.276(15)
Compound Er-3			
Cu(1)-N(7)	1.94(3)	Cu(1)-N(8)	2.00(2)
Cu(1)-N(6)	1.97(3)	Cu(1)-N(1)	2.02(3)
Cu(1)-O(29)	2.280(15)	Cu(2)-O(42)	2.321(14)
Cu(2)-N(21)	1.98(3)	Cu(2)-N(24)	2.05(2)
Cu(2)-N(23)	2.02(2)	Cu(2)-N(22)	2.07(3)
Cu(3)-N(19)	1.96(2)	Cu(3)-N(18)	1.99(2)
Cu(3)-N(20)	1.96(2)	Cu(3)-N(17)	2.01(3)
Cu(4)-N(11)	1.999(17)	Cu(4)-N(9)	2.03(3)
Cu(4)-N(12)	2.011(18)	Cu(4)-N(10)	2.064(16)
Cu(4)-O(2W)	2.374(16)	Cu(5)-O(3W)	2.411(18)
Cu(5)-N(13)	1.981(18)	Cu(5)-N(14)	2.02(2)
Cu(5)-N(16)	1.999(17)	Cu(5)-N(15)	2.028(17)
Cu(6)-N(5)	1.95(2)	Cu(6)-N(3)	1.97(2)
Cu(6)-N(4)	1.97(2)	Cu(6)-N(2)	1.987(19)
Er(1)-O(25)	2.257(15)	Er(1)-O(38)	2.322(13)
Er(1)-O(39)	2.259(14)	Er(1)-O(9W)	2.348(16)
Er(1)-O(31)	2.270(13)	Er(1)-O(41)	2.399(17)
Er(1)-O(35)	2.304(14)	Er(1)-O(115)	2.859(14)
Er(2)-O(76)	2.239(13)	Er(2)-O(10W)	2.380(17)
Er(2)-O(74)	2.261(14)	Er(2)-O(82)	2.383(13)

Er(2)-O(75)	2.263(14)	Er(2)-O(122)	2.397(17)
Er(2)-O(47)	2.279(17)	Er(2)-O(73)	2.863(14)
Si(2)-O(115)	1.602(15)	Si(2)-O(3)	1.630(15)
Si(2)-O(4)	1.628(13)	Si(2)-O(2)	1.636(13)
W(1)-O(14)	1.712(14)	W(1)-O(12)	1.928(13)
W(1)-O(16)	1.896(13)	W(1)-O(7)	1.937(14)
W(1)-O(15)	1.908(14)	W(1)-O(2)	2.332(14)
W(2)-O(5)	1.717(16)	W(2)-O(6)	1.916(14)
W(2)-O(8)	1.795(14)	W(2)-O(9)	1.953(12)
W(2)-O(7)	1.915(14)	W(2)-O(2)	2.349(13)
W(3)-O(10)	1.696(14)	W(3)-O(6)	1.924(15)
W(3)-O(11)	1.809(15)	W(3)-O(12)	1.937(14)
W(3)-O(13)	1.922(16)	W(3)-O(2)	2.368(12)
W(4)-O(18)	1.721(14)	W(4)-O(15)	1.883(14)
W(4)-O(20)	1.846(14)	W(4)-O(19)	1.942(15)
W(4)-O(17)	1.875(14)	W(4)-O(3)	2.401(14)
W(5)-O(22)	1.698(15)	W(5)-O(21)	1.932(13)
W(5)-O(23)	1.883(14)	W(5)-O(17)	1.949(15)
W(5)-O(13)	1.898(15)	W(5)-O(3)	2.354(13)
W(6)-O(27)	1.687(15)	W(6)-O(16)	1.924(12)
W(6)-O(28)	1.860(12)	W(6)-O(32)	1.932(13)
W(6)-O(19)	1.883(15)	W(6)-O(4)	2.390(13)
W(7)-O(33)	1.708(14)	W(7)-O(30)	1.929(11)
W(7)-O(34)	1.875(14)	W(7)-O(32)	1.965(13)
W(7)-O(9)	1.879(11)	W(7)-O(4)	2.350(12)
W(8)-O(37)	1.707(15)	W(8)-O(34)	1.949(13)
W(8)-O(35)	1.754(13)	W(8)-O(8)	2.050(13)
W(8)-O(36)	1.896(14)	W(8)-O(115)	2.277(14)
W(9)-O(40)	1.702(13)	W(9)-O(36)	1.959(14)
W(9)-O(39)	1.796(14)	W(9)-O(11)	2.037(15)
W(9)-O(23)	1.927(14)	W(9)-O(115)	2.305(14)
W(10)-O(24)	1.709(14)	W(10)-O(21)	1.950(13)
W(10)-O(25)	1.798(15)	W(10)-O(20)	2.084(14)
W(10)-O(26)	1.897(12)	W(10)-O(3)	2.328(14)
W(11)-O(31)	1.734(14)	W(11)-O(30)	1.931(13)
W(11)-O(29)	1.758(12)	W(11)-O(28)	2.025(14)
W(11)-O(26)	1.911(13)	W(11)-O(4)	2.311(11)
W(12)-O(42)	1.728(13)	W(12)-O(79)	1.932(13)
W(12)-O(76)	1.763(13)	W(12)-O(48)	2.026(14)
W(12)-O(44)	1.931(15)	W(12)-O(57)	2.356(12)
W(13)-O(43)	1.720(14)	W(13)-O(46)	1.948(13)
W(13)-O(47)	1.745(16)	W(13)-O(45)	2.029(13)
W(13)-O(44)	1.884(15)	W(13)-O(49)	2.341(14)

W(14)-O(69)	1.725(14)	W(14)-O(68)	1.962(16)
W(14)-O(75)	1.794(14)	W(14)-O(71)	1.999(14)
W(14)-O(72)	1.897(15)	W(14)-O(73)	2.312(13)
W(15)-O(80)	1.693(14)	W(15)-O(72)	1.950(16)
W(15)-O(74)	1.790(14)	W(15)-O(65)	2.064(16)
W(15)-O(56)	1.924(16)	W(15)-O(73)	2.318(13)
W(16)-O(70)	1.722(15)	W(16)-O(79)	1.929(13)
W(16)-O(71)	1.833(14)	W(16)-O(77)	1.944(14)
W(16)-O(67)	1.880(11)	W(16)-O(57)	2.294(14)
W(17)-O(78)	1.713(14)	W(17)-O(50)	1.928(14)
W(17)-O(48)	1.860(14)	W(17)-O(59)	1.928(12)
W(17)-O(77)	1.920(13)	W(17)-O(57)	2.379(13)
W(18)-O(53)	1.723(16)	W(18)-O(50)	1.905(14)
W(18)-O(45)	1.902(14)	W(18)-O(51)	1.919(15)
W(18)-O(54)	1.904(14)	W(18)-O(49)	2.396(14)
W(19)-O(52)	1.700(15)	W(19)-O(46)	1.924(13)
W(19)-O(55)	1.880(15)	W(19)-O(51)	1.929(14)
W(19)-O(56)	1.900(17)	W(19)-O(49)	2.332(13)
W(20)-O(66)	1.699(15)	W(20)-O(67)	1.968(12)
W(20)-O(68)	1.897(18)	W(20)-O(64)	1.980(14)
W(20)-O(63)	1.938(14)	W(20)-O(58)	2.374(13)
W(21)-O(62)	1.738(14)	W(21)-O(55)	1.941(15)
W(21)-O(65)	1.793(17)	W(21)-O(61)	1.957(16)
W(21)-O(63)	1.917(15)	W(21)-O(58)	2.332(12)
W(22)-O(60)	1.718(15)	W(22)-O(54)	1.898(15)
W(22)-O(64)	1.864(15)	W(22)-O(61)	1.929(15)
W(22)-O(59)	1.888(12)	W(22)-O(58)	2.378(13)
Compound Er-4			
Er(1)-O(14)	2.325(10)	Er(1)-O(55)	2.368(11)
Er(1)-O(22)	2.343(11)	Er(1)-O(69)	2.397(11)
Er(1)-O(30)	2.356(10)	Er(1)-O(72)	2.400(11)
Er(1)-O(24)	2.362(11)	Er(1)-O(7)	2.401(10)
Cu(1)-N(1)	1.970(14)	Cu(1)-N(4)	2.051(19)
Cu(1)-N(2)	2.006(13)	Cu(1)-N(3)	2.077(13)
Si(1)-O(29)	1.615(11)	Si(1)-O(80)	1.646(11)
Si(1)-O(19)	1.632(11)	Si(1)-O(77)	1.653(10)
Si(2)-O(2)	1.614(10)	Si(2)-O(28)	1.633(10)
Si(2)-O(35)	1.629(10)	Si(2)-O(73)	1.648(11)
W(1)-O(10)	1.704(11)	W(1)-O(78)	1.915(10)
W(1)-O(69)	1.797(10)	W(1)-O(34)	1.933(10)
W(1)-O(26)	2.111(10)	W(1)-O(35)	2.220(9)
W(2)-O(11)	1.722(10)	W(2)-O(78)	1.897(10)
W(2)-O(27)	1.893(10)	W(2)-O(20)	1.928(11)

W(2)-O(31)	1.894(11)	W(2)-O(2)	2.338(10)
W(3)-O(66)	1.733(13)	W(3)-O(13)	1.944(11)
W(3)-O(26)	1.837(10)	W(3)-O(91)	1.971(16)
W(3)-O(20)	1.902(10)	W(3)-O(28)	2.358(10)
W(4)-O(94)	1.730(12)	W(4)-O(50)	1.904(13)
W(4)-O(67)	1.878(11)	W(4)-O(91)	1.925(16)
W(4)-O(75)	1.898(11)	W(4)-O(28)	2.314(9)
W(5)-O(9)	1.707(10)	W(5)-O(13)	1.952(11)
W(5)-O(23)	1.817(11)	W(5)-O(75)	1.956(11)
W(5)-O(56)	1.950(12)	W(5)-O(28)	2.361(9)
W(6)-O(59)	1.704(11)	W(6)-O(27)	1.945(10)
W(6)-O(25)	1.829(11)	W(6)-O(67)	1.988(11)
W(6)-O(12)	1.921(11)	W(6)-O(2)	2.402(10)
W(7)-O(5)	1.748(10)	W(7)-O(33)	1.966(10)
W(7)-O(7)	1.788(11)	W(7)-O(23)	2.116(11)
W(7)-O(34)	1.939(10)	W(7)-O(35)	2.206(9)
W(8)-O(71)	1.702(11)	W(8)-O(31)	1.988(10)
W(8)-O(14)	1.756(10)	W(8)-O(25)	2.111(10)
W(8)-O(32)	1.924(10)	W(8)-O(2)	2.375(10)
W(9)-O(48)	1.711(11)	W(9)-O(74)	1.982(10)
W(9)-O(30)	1.753(10)	W(9)-O(53)	2.111(11)
W(9)-O(32)	1.907(10)	W(9)-O(73)	2.320(11)
W(10)-O(47)	1.728(10)	W(10)-O(74)	1.917(11)
W(10)-O(56)	1.873(12)	W(10)-O(15)	1.923(11)
W(10)-O(33)	1.882(10)	W(10)-O(73)	2.327(9)
W(11)-O(43)	1.722(10)	W(11)-O(15)	1.930(10)
W(11)-O(53)	1.820(12)	W(11)-O(50)	1.963(13)
W(11)-O(12)	1.886(10)	W(11)-O(73)	2.401(10)
W(12)-O(42)	1.708(11)	W(12)-O(79)	1.911(11)
W(12)-O(57)	1.899(16)	W(12)-O(70)	1.917(11)
W(12)-O(37)	1.904(13)	W(12)-O(77)	2.324(10)
W(13)-O(95)	1.750(12)	W(13)-O(44)	1.959(12)
W(13)-O(72)	1.762(11)	W(13)-O(4)	2.110(12)
W(13)-O(57)	1.941(16)	W(13)-O(29)	2.213(10)
W(14)-O(1)	1.711(11)	W(14)-O(70)	1.939(11)
W(14)-O(24)	1.766(12)	W(14)-O(76)	2.095(10)
W(14)-O(16)	1.915(10)	W(14)-O(77)	2.339(10)
W(15)-O(93)	1.724(11)	W(15)-O(68)	1.924(13)
W(15)-O(4)	1.830(12)	W(15)-O(49)	1.970(11)
W(15)-O(79)	1.919(11)	W(15)-O(80)	2.368(10)
W(16)-O(38)	1.731(11)	W(16)-O(37)	1.946(12)
W(16)-O(76)	1.830(11)	W(16)-O(21)	1.958(11)
W(16)-O(51)	1.900(12)	W(16)-O(77)	2.394(10)

W(17)-O(45)	1.715(13)	W(17)-O(8)	1.911(11)
W(17)-O(21)	1.893(11)	W(17)-O(81)	1.921(10)
W(17)-O(49)	1.895(12)	W(17)-O(80)	2.314(10)
W(18)-O(46)	1.763(12)	W(18)-O(52)	1.941(11)
W(18)-O(55)	1.774(11)	W(18)-O(54)	2.089(11)
W(18)-O(44)	1.908(12)	W(18)-O(29)	2.249(10)
W(19)-O(17)	1.721(11)	W(19)-O(3)	1.971(11)
W(19)-O(22)	1.749(10)	W(19)-O(18)	2.100(11)
W(19)-O(16)	1.951(10)	W(19)-O(19)	2.381(10)
W(20)-O(92)	1.737(12)	W(20)-O(68)	1.955(11)
W(20)-O(54)	1.824(12)	W(20)-O(81)	1.973(10)
W(20)-O(60)	1.930(11)	W(20)-O(80)	2.320(11)
W(21)-O(58)	1.724(12)	W(21)-O(8)	1.935(11)
W(21)-O(18)	1.828(11)	W(21)-O(6)	1.945(10)
W(21)-O(51)	1.908(11)	W(21)-O(19)	2.395(10)
W(22)-O(39)	1.706(11)	W(22)-O(60)	1.915(10)
W(22)-O(3)	1.875(11)	W(22)-O(6)	1.941(11)
W(22)-O(52)	1.881(11)	W(22)-O(19)	2.330(10)

Symmetry transformations used to generate equivalent atoms: Symmetry transformations used to generate equivalent atoms: For **Dy-1** #1 x, y, z+1; #2 x, -y+1, z; #3 x, y, z-1.

Reference:

1. A. Tézé, G. Hérvé, *Inorganic Synthesis*, Wiley, New York, 1990.

2. G. M. Sheldrick, SADABS; University of Göttingen: Germany, 1996.

3. (a) G. M. Sheldrick, SHELXS-97, Program for X-ray Crystal Structure Determination; University of Gottingen: Germany, 1997; (b) G. M. Sheldrick, SHELXL-97, Program for X-ray Crystal Structure Refinement; University of Gottingen: Germany, 1997; (c) CrystalClear, version 1.3.5; Rigaku Corp.: Woodlands, TX, 1999; (d) G. M. Sheldrick, SHELX-96: Program for Crystal Structure Determination; Siemens Analytical X-ray Instruments: Madison, WI, 1996.